

T.R.N.C
NEAR EAST UNIVERSITY
GRADUATE SCHOOL OF HEALTH SCIENCES

INHIBITORY EFFECT OF FLUOXETINE ON
GLUTATHIONE REDUCTASE PURIFIED FROM
BAKER'S YEAST

Evelyn BRIGHT ASUQUO

MEDICAL BIOCHEMISTRY PROGRAM

MASTER OF SCIENCE THESIS

NICOSIA

2017

T.R.N.C.
NEAR EAST UNIVERSITY
GRADUATE SCHOOL OF HEALTH SCIENCES

**INHIBITORY EFFECT OF FLUOXETINE ON
GLUTATHIONE REDUCTASE PURIFIED FROM
BAKER'S YEAST**

Evelyn BRIGHT ASUQUO

MEDICAL BIOCHEMISTRY PROGRAM
MASTER OF SCIENCE THESIS

SUPERVISOR
Associate Professor Özlem DALMIZRAK

NICOSIA
2017

The Directorate of Graduate School of Health Science,

This study has been accepted by the Thesis committee in Medical Biochemistry Program as Master Thesis.

Thesis committee:

Chair: Professor Nazmi ÖZER
Near East University

Member: Professor Nevbahar TURGAN
Ege University

Supervisor: Associate Professor Özlem DALMIZRAK
Near East University

Approval:

According to the relevant articles of Near East University Postgraduate Study – Education and Examination Regulations, this thesis has been approved by the above mentioned members of the thesis committee and the decision of the Board of Directors of the Institute.

.

Prof. Dr. İhsan ÇALIŞ
Director of Graduate School of Health Sciences

ACKNOWLEDGEMENTS

First and foremost, in a very special way, I would like to express my profound gratitude to my supervisor Assoc. Prof. Dr. Özlem Dalmızrak for her contribution, encouragement, advice, corrections, patience and support throughout my postgraduate study.

I am most grateful to Prof. Dr. Nazmi Özer for his guidance and support during my thesis and academic study.

I am grateful to Prof. Dr. İ Hamdi Ögüş for his contributions.

I would like to thank my course mates in the Department of Medical Biochemistry for their support and encouragement throughout my thesis study. Most importantly I would like to thank my colleague Redwan Kawa for his assistance and friendly support throughout my thesis year.

In a special way, I would like to thank my friends for their friendly encouragements during my thesis study.

Finally, in a remarkable way, I would like to thank my parents Mr. and Mrs. Bright Asuquo for their financial support, love and care throughout my years of education.

ABSTRACT

Asuquo E.B. Inhibitory Effect of Fluoxetine on Glutathione Reductase Purified from Baker's Yeast. Near East University, Graduate School of Health Sciences, M.Sc. Thesis in Medical Biochemistry Program, Nicosia, 2017.

Glutathione reductase (E.C. 1.6.4.2) from baker's yeast (*S. cerevisiae*) is a homodimeric enzyme and plays a central role in detoxification since it regenerates the central antioxidant molecule, reduced glutathione (GSH), from oxidized glutathione (GSSG) in expense of a mole of NADPH. GSH scavenges and eliminates superoxide and hydroxyl radicals non-enzymatically or functions as an electron donor for several enzymes. In this study, we investigated the interaction of fluoxetine, an antidepressant, with glutathione reductase (GR). Determination of the optimum temperature and optimum pH were performed in 100 mM phosphate buffer pH 7.5 containing 0.1 mM NADPH and 1 mM GSSG. In the presence of fluoxetine, glutathione reductase activity was followed at fixed 1 mM [GSSG]-variable [NADPH] and at fixed 0.1 mM [NADPH]-variable [GSSG]. GR gave single protein and activity bands on native PAGE. It also gave single band on SDS-PAGE with Mr of 49 kDa. Optimum pH, optimum temperature, activation energy and Q_{10} were found as 7.65, 57°C, 3,544 calories and 1.26, respectively. Fluoxetine inhibited GR in a dose dependent manner and IC_{50} was calculated as 0.73 mM. When the variable substrate was GSSG, inhibition of GR by fluoxetine was linear-mixed type competitive with a K_s , K_i and α values of $111 \pm 5 \mu\text{M}$, $279 \pm 32 \mu\text{M}$ and 5.48 ± 1.29 , respectively. On the other hand, at variable NADPH, the inhibition type was noncompetitive, K_m and K_i values were $13.4 \pm 0.8 \mu\text{M}$ and $879 \pm 82 \mu\text{M}$, respectively. Linear-mixed type competitive and noncompetitive inhibitions suggest that fluoxetine binds neither GSSG nor NADPH sites rather it binds to a site between GSSG and NADPH binding sites and much closer to the GSSG site. Thus, it competes with GSSG binding but then noncompetitive inhibition with variable NADPH can be explained by the conformational change of the enzyme.

Keywords: Glutathione reductase, fluoxetine, inhibition kinetics, K_i

ÖZET

Asuquo E.B. Fluoksetinin Ekmek Mayasından Saflaştırılan Glutasyon Redüktaz Enzimine İnhibe Edici Etkisi. Yakın Doğu Üniversitesi, Sağlık Bilimleri Enstitüsü, Tıbbi Biyokimya Programı, Yüksek Lisans Tezi, Lefkoşa, 2017.

Ekmek mayasından (*S. cerevisiae*) elde edilen glutasyon redüktaz (E.C. 1.6.4.2) homodimerik bir enzimdir ve okside glutasyonu (GSSG) bir mol NADPH harcayarak antioksidan bir molekül olan redükte glutatyona (GSH) çevirdiği için detoksifikasyonda önemli rol oynamaktadır. GSH non-enzimatik olarak süperoksit ve hidroksil radikallerini ortadan kaldırmakta ve birçok enzim için elektron vericisi olarak görev yapmaktadır. Çalışmada antidepresan olan fluoksetinin glutasyon redüktaz (GR) ile etkileşimi incelenmiştir. Optimum sıcaklık ve optimum pH tayini 0.1 mM NADPH ve 1 mM GSSG içeren 100 mM fosfat tamponu (pH 7.5) kullanılarak yapılmıştır. Glutasyon redüktaz aktivitesi fluoksetin varlığında sabit 1 mM [GSSG]-değişken [NADPH] ve sabit 0.1 mM [NADPH]-değişken [GSSG] kullanılarak ölçülmüştür. Natif-PAGE'de GR'ye ait tek bir protein ve aktivite bandı elde edilmiştir. SDS-PAGE'de molekül ağırlığı 49 kDa olarak hesaplanan tek bir bant elde edilmiştir. Optimum pH, optimum sıcaklık, aktivasyon enerjisi ve Q_{10} sırasıyla 7.65, 57°C, 3,544 kalori ve 1.26 olarak bulunmuştur. Fluoksetin GR'yi doza bağımlı olarak inhibe etmektedir. IC_{50} 0.73 mM olarak hesaplanmıştır. Değişken substrat GSSG olduğunda fluoksetin GR'yi lineer karışık tip kompetitif olarak inhibe etmektedir. K_s , K_i ve α değerleri sırasıyla $111 \pm 5 \mu\text{M}$, $279 \pm 32 \mu\text{M}$ and 5.48 ± 1.29 olarak bulunmuştur. Diğer yandan, değişken substrat NADPH olduğunda inhibisyon tipi non-kompetitiftir. K_m ve K_i değerleri sırasıyla $13.4 \pm 0.8 \mu\text{M}$ ve $879 \pm 82 \mu\text{M}$ olarak hesaplanmıştır. Lineer karışık tip kompetitif ve non-kompetitif inhibisyon, fluoksetinin GSSG veya NADPH bağlanma bölgelerine bağlanmadığını, bu bölgelerin arasındaki bir bölgeye ve de GSSG bağlanma bölgesine daha yakın olacak şekilde bağlandığını göstermektedir. Dolayısıyla fluoksetin GSSG ile yarışmaktadır. Ayrıca değişken NADPH ile gözlenmiş olan non-kompetitif inhibisyon da enzimdeki konformasyonel değişiklik ile açıklanabilmektedir.

Anahtar Kelimeler: Glutasyon redüktaz, fluoksetin, inhibisyon kinetiği, K_i

TABLE OF CONTENTS

	Page No
APPROVAL	iii
ACKNOWLEDGEMENTS	iv
ABSTRACT	v
ÖZET	vi
TABLE OF CONTENTS	vii
ABBREVIATIONS	ix
LIST OF FIGURES	xi
LIST OF TABLES	xiii
1. INTRODUCTION	1
2. GENERAL INFORMATION	3
2.1. Antioxidant Enzymes	3
2.1.1. Glutathione Reductase	3
2.1.2. Glutathione Peroxidase	3
2.1.3. Superoxide Dismutase	4
2.1.4. Catalase	5
2.2. Glutathione Reductase in Erythrocytes and Hepatocytes	6
2.3. Catalytic Mechanism of Glutathione Reductase	8
2.4. Glutathione: Structure, Function and Role in Antioxidant System	9
2.5. Biosynthesis of Glutathione	11
2.6. Functions of Glutathione and Glutathione Reductase	11
2.7. Antioxidant Mechanism of Glutathione	12
2.8. Reactive Oxygen Species	13
2.9. Sources of Reactive Oxygen Species	13
2.10. Oxidative Stress	14
2.11. The Role of Glutathione Reductase in Oxidative Stress Related Diseases	15
2.12. Fluoxetine	17
3. MATERIALS AND METHODS	19
3.1. Chemicals	19
3.2. Methods	19
3.2.1. Preparation of Glutathione Reductase	19

3.2.2. Determination of Protein Concentration	19
3.2.3. Native-Polyacrylamide Gel Electrophoresis (Native-PAGE)	20
3.2.4. Sodium Dodecyl Sulfate-Polyacrylamide Gel Electrophoresis (SDS-PAGE)	23
3.2.5. Coomassie Brilliant Blue (CBB) R-250 Staining	25
3.2.6. Silver Staining	26
3.2.7. Activity Staining	26
3.2.8. Measurement of Glutathione Reductase Enzyme Activity	26
3.2.9. Determination of Optimum pH	27
3.2.10. Determination of Optimum Temperature	28
3.2.11. Effect of Fluoxetine on Glutathione Reductase Enzyme Activity	28
3.2.12. Inhibitory Kinetic Experiments with Fluoxetine	28
3.2.13. Statistical Analysis	29
4. RESULTS	30
4.1. Determination of Protein Concentration	30
4.2. Characterization of Glutathione Reductase Enzyme	30
4.2.1. Purity Control of Glutathione Reductase Enzyme	30
4.2.2. Zero Buffer Extrapolation and Determination of Optimum pH	34
4.2.3. Determination of Optimum Temperature	36
4.3. Substrate Kinetics	36
4.4. Inhibitory Kinetic Behaviour of GR with Fluoxetine	40
5. DISCUSSION	51
6. CONCLUSION	57
REFERENCES	58

ABBREVIATIONS

ADP	: Adenosine diphosphate
AP-1	: Activator protein 1
APS	: Ammonium persulphate
ATP	: Adenosine triphosphate
BSA	: Bovine serum albumin
BPB	: Bromophenol blue
β -ME	: Beta-mercaptoethanol
CAT	: Catalase
CBB	: Coomassie brilliant blue
CYP	: Cytochrome P450
DMSO	: Dimethyl sulfoxide
DNA	: Deoxyribonucleic acid
E_a	: Energy of activation
E.C.	: Enzyme commission number
FAD	: Flavin adenine dinucleotide
G6PD	: Glucose-6-phosphate dehydrogenase
GCL	: Glutamate cysteine ligase
GPx	: Glutathione peroxidase
GR	: Glutathione reductase
GSH	: Reduced glutathione
GSSG	: Oxidized glutathione
GST	: Glutathione-S-transferase
H ₂ O ₂	: Hydrogen peroxide
IC_{50}	: Half maximum inhibitory velocity
kDa	: kilo Dalton
K_i	: Inhibitory constant
K_m	: Michaelis constant
K_s	: Dissociation constant
M_r	: Molecular weight
MTT	: Thiazolyl blue tetrazolium bromide
NADP ⁺	: Nicotinamide adenine dinucleotide (oxidized form)

NADPH	: Nicotinamide adenine dinucleotide (reduced form)
Native-PAGE	: Native-polyacrylamide gel electrophoresis
NF-kB	: Nuclear factor-kappa B
$\cdot\text{OH}$: Hydroxyl radical
$\text{O}_2^{\cdot-}$: Superoxide anion
OCD	: Obsessive compulsive disorder
PD	: Parkinson's disease
6-PGD	: 6-Phosphogluconate dehydrogenase
Q_{10}	: Temperature coefficient
RBC	: Red blood cells
RNS	: Reactive nitrogen species
ROS	: Reactive oxygen species
SCA	: Sickle cell anemia
SDS-PAGE	: Sodium dodecyl sulphate polyacrylamide gel electrophoresis
SOD	: Superoxide dismutase
SP-1	: Specificity protein 1
SNPc	: Substantia nigra pars compacta
SSRI	: Selective serotonin re-uptake inhibitor
TAS	: Total antioxidant status
TEMED	: N, N, N,'N'- Tetramethylenediamine
Tris	: Tris(hydroxymethyl) aminomethane
V_m	: Maximum velocity

LIST OF FIGURES

	Page No
Figure 1.1. Reduction of oxidized glutathione to reduced glutathione by glutathione reductase	2
Figure 2.1. Glutathione reductase action in the presence of ROS	3
Figure 2.2. Action of GPx and GR in the oxidation and reduction of glutathione	4
Figure 2.3. Reaction catalyzed by superoxide dismutase	4
Figure 2.4. Reaction catalyzed by catalase	5
Figure 2.5. Antioxidant defense mechanism	6
Figure 2.6. Structure of glutathione reductase	7
Figure 2.7. Glutathione reductase action during aerobic glycolysis	8
Figure 2.8. Glutathione reductase catalytic cycle	9
Figure 2.9. Structure of reduced and oxidized glutathione	10
Figure 2.10. Biosynthesis of glutathione	11
Figure 2.11. Antioxidant mechanism of glutathione	13
Figure 2.12. Production and effects of ROS	14
Figure 2.13. Schematic presentation of ROS mechanism and damage	15
Figure 2.14. Structures of fluoxetine and norfluoxetine enantiomers	18
Figure 4.1. Determination of the enzyme concentration by Bradford assay	30
Figure 4.2. Glutathione reductase enzyme on discontinuous native-PAGE	31
Figure 4.3. Silver staining of glutathione reductase on native-PAGE	32
Figure 4.4.A. Visualization of GR enzyme on discontinuous SDS-PAGE by the use of Coomassie Brilliant Blue staining	33
Figure 4.4.B. Log (Mr) vs R _f plot	33
Figure 4.5. Visualization of GR enzyme on discontinuous SDS-PAGE by the use of silver staining	34
Figure 4.6. ΔA/min vs buffer concentration	35
Figure 4.7. ΔA/min vs. pH plot	35
Figure 4.8.A. Specific activity vs. temperature plot	37
Figure 4.8.B. Log (Sp.Act.) U/mg protein vs. 1/T plot	37
Figure 4.9. Kinetic behavior of glutathione reductase with variable	

	GSSG concentrations	38
Figure 4.10.	Kinetic behavior of glutathione reductase with variable NADPH concentrations	39
Figure 4.11.	Dose dependent inhibition of glutathione reductase by fluoxetine	40
Figure 4.12.	Michaelis-Menten plot for glutathione reductase enzyme with different concentrations of fluoxetine using GSSG as a variable substrate	41
Figure 4.13.	Lineweaver-Burk plot for glutathione reductase enzyme at different concentrations of fluoxetine by using GSSG as a variable substrate	42
Figure 4.14.	Replot of slope and intercept points versus fluoxetine obtained from Figure 4.13	43
Figure 4.15.	Dixon plot for glutathione reductase enzyme at different concentrations of fluoxetine by using GSSG as variable a substrate	44
Figure 4.16.	Replot of slopes obtained from Figure 4.15 versus $1/[GSSG]$	45
Figure 4.17.	Michaelis-Menten plot for glutathione reductase enzyme at different concentrations of fluoxetine by using NADPH as a variable substrate	46
Figure 4.18.	Lineweaver-Burk plot for glutathione reductase enzyme at different concentrations of fluoxetine by using NADPH as a variable substrate	47
Figure 4.19.	Replot of slope and intercept points obtained from Figure 4.18 versus [fluoxetine]	48
Figure 4.20.	Dixon plot for glutathione reductase enzyme at different concentrations of fluoxetine by using NADPH as a variable substrate	49
Figure 4.21.	Replot of slopes obtained from Figure 4.20 versus $1/[NADPH]$	50

LIST OF TABLES

		Page No
Table 3.1.	Volume used in gel preparation of Native-PAGE	21
Table 3.2.	Volume used in gel preparation of SDS-PAGE	24

1. INTRODUCTION

Glutathione reductase (E.C. 1.6.4.2) is an antioxidant enzyme present in virtually all living cells and organs especially in the erythrocytes and hepatocytes of the living system (Arora et al., 2013). Its comprehensive function is to maintain a reduced state of the cell by its action in the elimination of free radicals, prevention of oxidative stress and lipid peroxidation (Ray et al., 2014). This enzyme can also be found in numerous microorganisms, yeast, plants and animals (Krauth-Siegel et al., 1982). Its impairment can result in oxidative stress and in prolonged cases apoptosis (Zhao et al., 2009).

Glutathione reductase (GR) is a dimeric enzyme and is associated with the flavoprotein family. Consisting of two identical subunits, each of its subunits contains a mole of non-covalently bound nicotinamide adenine dinucleotide phosphate (NADPH) and flavin adenine dinucleotide (FAD) (Berkholz et al., 2008). GR is essential in detoxification owing to the fact that it regenerates the leading antioxidant molecule glutathione (GSH) from its oxidized form (GSSG) at the expense of a mole of reduced nicotinamide adenine dinucleotide phosphate (NADPH) (Kaneko et al., 2002).

GR is linked to the NADPH-dependent oxidoreductase family. Its main action is in the conservation of a steady level of reduced glutathione (GSH) in the living system. GSH is an essential molecule in the elimination of reactive oxygen species (ROS) thereby protecting the cells against oxidative stress. GR plays a paramount role in glutathione metabolism by catalyzing the reduction of GSSG to its reduced form GSH using NADPH as a reducing agent. GSH destroys free radicals ((superoxide (O_2^-) and hydroxyl radicals (OH^\cdot)) non-enzymatically or by acting as an electron donor to certain antioxidant enzymes involved in the destruction of ROS (Pannala et al., 2013). When, GSH is oxidized to GSSG by glutathione peroxidase, GR regenerates GSH using the reducing power of NADPH. (Figure 1.1) (Arora et al., 2013).

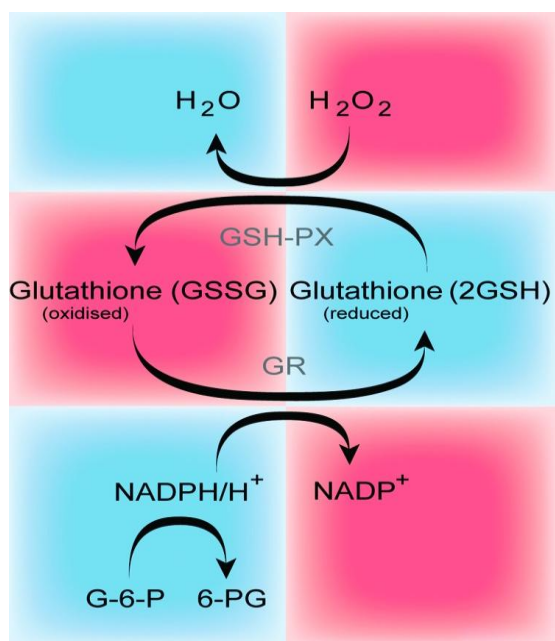


Figure 1.1. Reduction of oxidized glutathione to reduced glutathione by glutathione reductase (Olschewski and Weir, 2015).

Fluoxetine, an antidepressant, is a re-uptake inhibitor of the monoamine neurotransmitter, serotonin (Johnson et al., 2007). It is mostly taken orally and widely distributed in the blood, liver and other tissues. Fluoxetine is known to have an inhibitory effect on glutathione reductase (Adzic et al., 2011).

The objective of this study was to elucidate the inhibition kinetics of baker's yeast GR by fluoxetine. In this study, first the characterization of the GR was performed; subunit molecular weight, optimum pH and optimum temperature was determined. Then in the presence of varying concentrations of GSSG, NADPH and fluoxetine, the kinetic behavior of GR was elucidated.

2. GENERAL INFORMATION

2.1. Antioxidant Enzymes

Antioxidant enzymes are very crucial in the removal of reactive oxygen species (ROS), because they catalyze the breakdown of ROS and thus prevent their damaging roles to the cells (Tokarz et al., 2013). Therefore, the living organisms are in a continuous combat with ROS, to relief the negative effects of these species. Antioxidant enzymes are virtually present in all cells. Each of these enzymes has a distinctive role in the elimination of ROS (Birben et al., 2012).

2.1.1. Glutathione Reductase

Glutathione reductase (GR) plays a primary role in maintaining an appropriate level of reduced glutathione (GSH) through the conversion of oxidized glutathione disulphide (GSSG) to reduced glutathione. The reduced glutathione thereby eliminates the ROS present in cells. In normal cases, due to the fact that ROS are produced as a result of normal aerobic activities in the cell. The cell therefore develops a matrix of destructive enzymes to eliminate the ROS (Pannala et al., 2013). In the mechanism of GR, NADPH is required as a reducing factor to produce GSH which is a very important scavenging molecule that eliminates the ROS hence protecting the cells against damage (Figure 2.1) (Zhao et al., 2009).

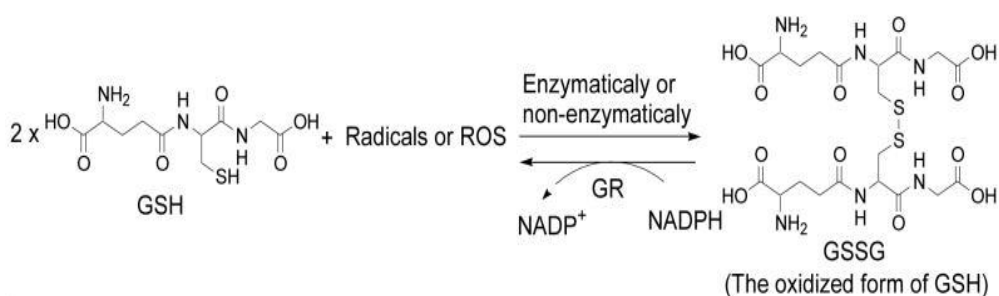


Figure 2.1. Glutathione reductase action in the presence of ROS (Zhao et al., 2009)

2.1.2. Glutathione Peroxidase

Glutathione peroxidase (GPx) is an important enzyme of the antioxidant system, in other words, it is known to be the main scavenging enzyme that destroys

hydrogen peroxide by using GSH as a substrate (Toppo et al., 2009). Glutathione using enzymes exist in two forms; the selenium dependent form known as glutathione peroxidases (GPx) and the selenium independent form known as glutathione-S-transferases (GSTs). The dissimilarities between GPx and GST are the presence of selenium at the active site of GPx and thiol at the active site of GST and their catalytic mechanisms. GPx converts hydrogen peroxide (H_2O_2) to water by using GSH as a co-substrate and oxidizing it to GSSG (Rahman, 2007). For GPx to carry out an optimum activity, GR has to maintain a continuous production of GSH from GSSG (Figure 2.2) (Day, 2009).



Figure 2.2. Action of GPx and GR in the oxidation and reduction of glutathione (Weydert and Cullen, 2010)

2.1.3. Superoxide Dismutase

Superoxide dismutases (SOD) belong to the family of metalloenzymes. Their distinctive role in protecting the cell against oxidative injury is mediated by accepting and donating electrons thereby forming hydrogen peroxide through the disintegration of superoxide anion (Figure 2.3) (Nojima et al., 2015). Destructive hydrogen peroxide compound is then eliminated by the other antioxidant enzymes like the glutathione peroxidase and catalase (Weydert and Cullen, 2010). SOD is one of the most valuable antioxidant enzymes in the living cells, it exists in different isoforms which vary in their amino acid compositions and active metal centers. In mammalian cells, SOD is found in three forms: SOD1 (Cu, Zn-SOD) is found in the cytoplasm, SOD2 (Mn-SOD) found in the mitochondria and SOD3 (Cu and Zn-SOD), known as the extracellular SOD (Rahman, 2007). SOD1 and SOD3 contain copper and zinc while SOD2 contains manganese (Lobo et al., 2010).

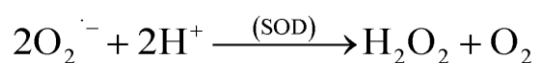


Figure 2.3. Reaction catalyzed by superoxide dismutase

2.1.4. Catalase

Catalase (CAT) is also important in the antioxidant system, it requires NADPH in order to remain in its active form (Birben et al., 2012). It is found in the peroxisomes, its main function is to convert hydrogen peroxide into water and oxygen (Figure 2.4). Hydrogen peroxide is produced in cells during normal daily body metabolism. It is known to be harmful to the cells and the organism tries to avert the damaging effect of this by-product by converting it into harmless substances. (Lobo et al., 2010).

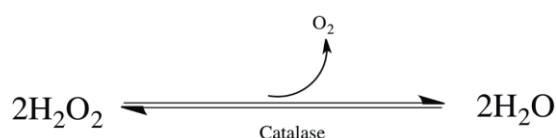


Figure 2.4. Reaction catalyzed by catalase

Other antioxidant enzymes like glutathione-S-transferase (GST) and glucose-6-phosphate dehydrogenase (G6PD) also eliminate ROS in different ways by reducing lipid peroxidation through selenium independent glutathione peroxidase (GPx) (Sharma et al., 2004) and the production of reduced nicotinamide adenine dinucleotide phosphate (NADPH), respectively for defense against oxidative injury (Abdul-Razzak et al., 2008).

All enzymes of the antioxidant defense system work together in a very coordinated way, with the sole purpose of eliminating ROS to avoid oxidative injury (Figure 2.5). Superoxide dismutase (SOD) and reactive oxygen species (ROS) generate hydrogen peroxide (H_2O_2) through their different activities. Due to an increase in H_2O_2 formation, cells produce the antioxidant enzymes GPx and CAT to remove the hydrogen peroxide thereby neutralizing its hazardous effects. The biosynthesis of the scavenging molecule GSH is also increased through GR activity which functions as a co substrate for GPx and GST. G6PD is also very essential in the antioxidant defense system, through the pentose phosphate pathway, a substantial amounts of reduced NADPH is generated by G6PD action (Weydert and Cullen, 2010).

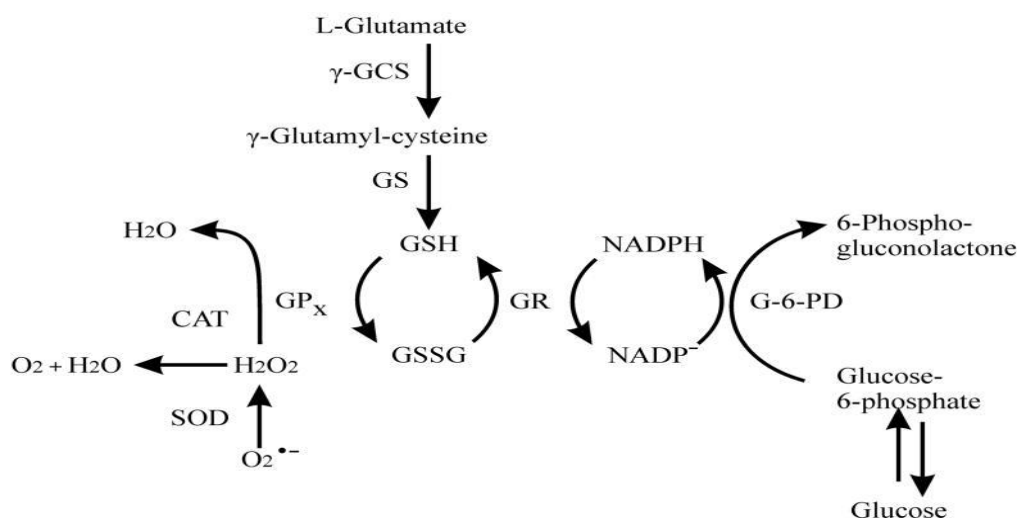


Figure 2.5. Antioxidant defense mechanism (Weydert and Cullen, 2010)

2.2. Glutathione Reductase in Erythrocytes and Hepatocytes

The homodimer flavoenzyme GR is very essential in the red blood cells (RBC) with a sole purpose of protecting the erythrocytes' enzymes, biological cell membrane and most importantly hemoglobin against oxidative injury (Chang et al., 1978). Hemoglobin, a protein molecule found in the erythrocytes is very crucial in the transportation of oxygen throughout the body. The protein GR ensures that hemoglobin molecule is properly protected against oxidative damage. In the RBCs, GR generates reduced glutathione with the help of NADPH as a reducing cofactor derived from the hexose monophosphate pathway (Beutler, 1969).

GR, present in the mammalian cells, has two identical subunits and its active site is formed by the residues of both subunits, suggesting that each monomer is not active on its own (Kamerbeek et al., 2007) (Figure 2.6).

In human, the gene encoding GR is a single gene called glutathione disulphide reductase gene (*GSR gene*). The *GSR gene* is made up of two in frame start codons which are known to generate mitochondrial and cytosolic GR (Outten and Culotta, 2004).

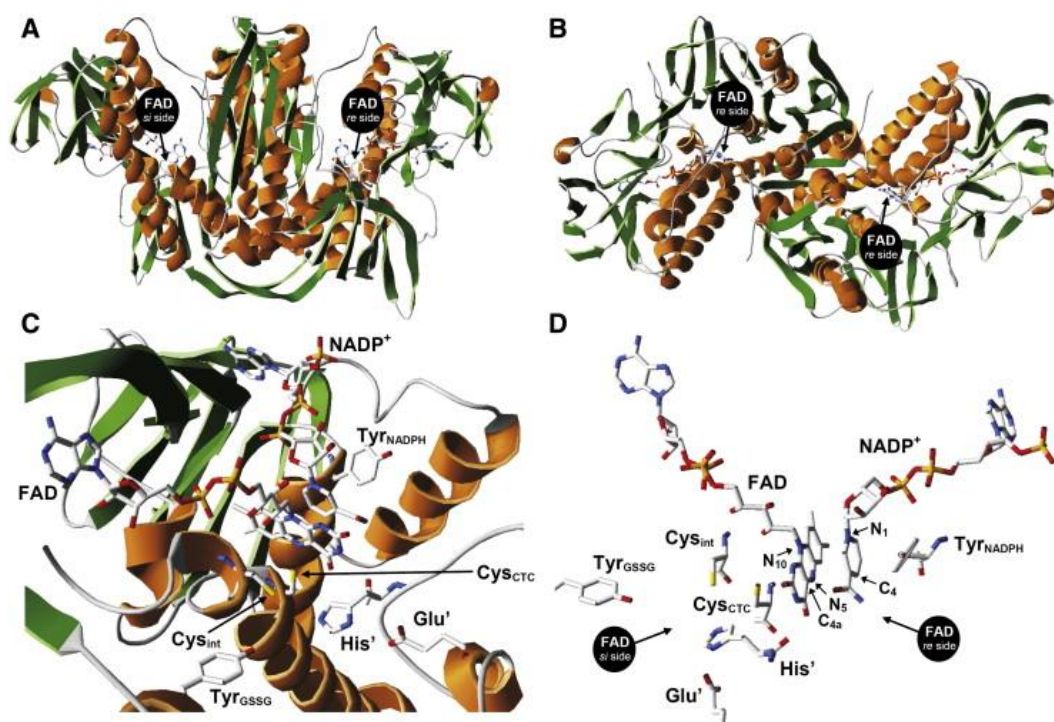


Figure 2.6. Structure of glutathione reductase. A. Front view of the homodimeric subunit contains flavin adenine dinucleotide (FAD) molecule bound per subunits. The opposite sides of the flavins (si and re side) are shown. B. NADPH is bound to re side of the FAD. This view particularly at the top shows a cleft at the re side revealing the binding site for FAD and NADPH. The protein backbones are shown as ribbons. Each subunit contains catalytic sites for both subunits. C. The GSSG binding site is comprised of both monomers. D. Spatial arrangement of substrate binding sites (Deponte, 2013).

In RBCs, NADPH is synthesized from glucose by the consecutive action of two enzymes of pentose phosphate pathway; glucose-6-phosphate dehydrogenase (G6PD) and 6-phosphogluconate dehydrogenase (6-PGD), to donate NADPH to GR to maintain GSH level (Figure 2.7). In a situation, where GR is unable to maintain GSH level in the RBCs, this can lead to H_2O_2 accumulation and cell membrane breakdown thereby resulting to hemolysis. Therefore the deficiency of GR can lead to moderately severe or mild anemia. This is the situation observed in G6PD deficiency (Chang et al., 1978).

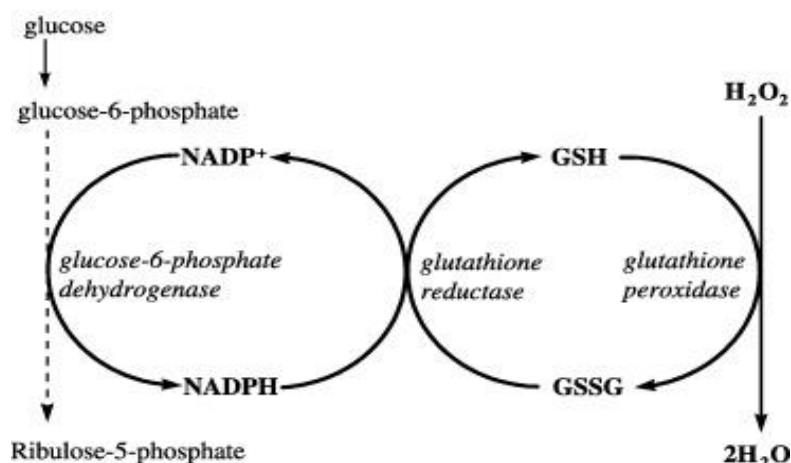


Figure 2.7. Glutathione reductase action during aerobic glycolysis (Matthews and Butler, 2005).

2.3. Catalytic Mechanism of Glutathione Reductase

In the reductive half reaction, FAD molecule which is bound to one of the subunit of the GR enzyme is reduced to FADH⁻ by NADPH. Electrons at this point are transferred from FADH⁻ to the redox active disulphide and NADPH is converted NADP⁺. The FADH⁻ anion formed by this reaction breaks disulphide bonds of GR (Cys₅₈-Cys₆₃). GR disulphide in its oxidized form binds and forms one mixed disulphide. This mixed disulphide is formed with Cys₅₈ together with the reduced GR enzyme which is bound by the oxidized glutathione enzyme. At this point, the mixed disulphide on Cys₅₈ is attacked by Cys₆₈ to release another reduced glutathione thereby forming an active disulphide. Through this redox mechanism containing GSSG and NADPH, two glutathione molecules in their reduced forms are generated (Figure 2.8) (Rietveld et al., 1994; Berkholz et al., 2008).

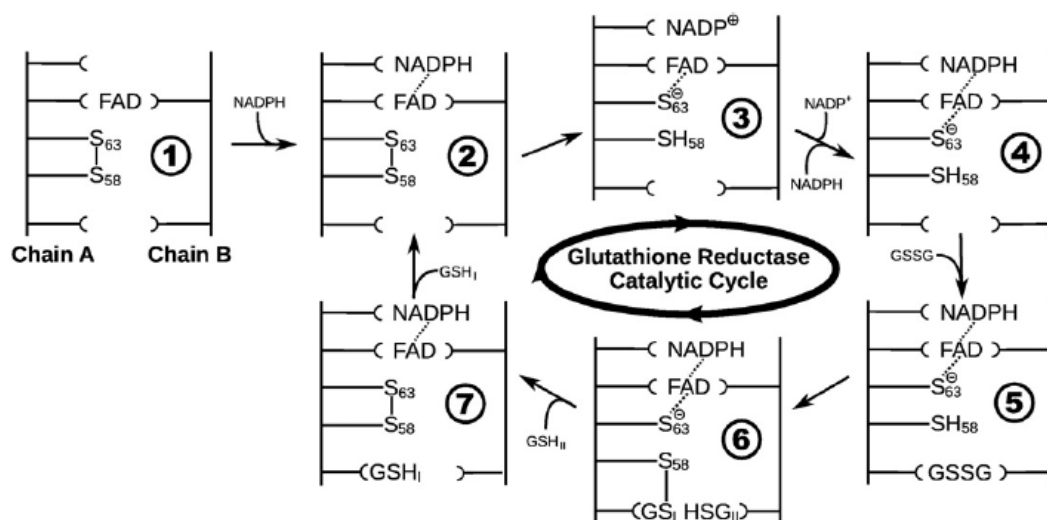


Figure 2.8. Glutathione reductase catalytic cycle (Berkholz et al., 2008)

2.4. Glutathione: Structure, Function and Role in Antioxidant System

Glutathione (GSH) is simply a protective molecule against ROS. It plays a vital role in the antioxidant defense system. GSH is found in tissues of all mammals, plants and even certain bacteria and yeasts. All mammalian tissues contain the tripeptide glutathione molecule, highest concentrations in the liver making it the key molecule in elimination of xenobiotics, programmed cell death, cell proliferation modulator, protein redox signaling etc. (Lu, 2013).

Glutathione exists in two forms, the oxidized and the reduced form. The oxidized glutathione (GSSG) which consists of disulphide linkage that binds the two glutathione monomers together, is actually the inactive form of glutathione due to the fact that without the action of GR, its accumulation may facilitate the harmful effects of ROS in the body. Its oxidized part (GSSG) is less than 1% of the reduced form (GSH) which happens to be the active and very essential form of glutathione since it is the main antioxidant and scavenging molecule (Figure 2.9). In eukaryotes, cellular GSH predominates in the cytosol at about 90%, only 10% is found in the mitochondria and little amounts in the endoplasmic reticulum (Lu, 2009).

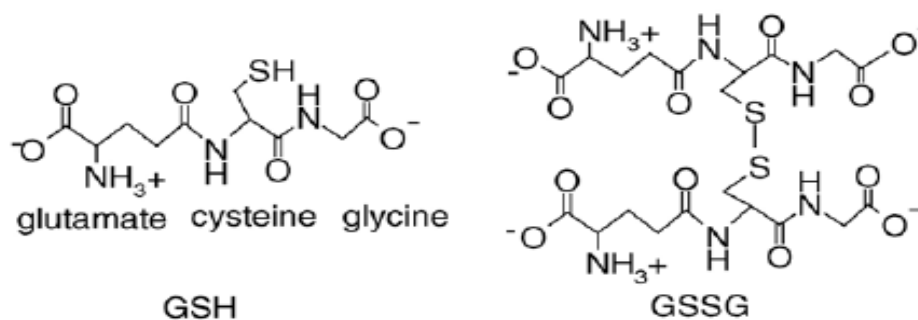


Figure 2.9. Structure of reduced and oxidized glutathione (Valko et al., 2006)

The tripeptide GSH molecule is generated and recycled in all mammalian cells. It is composed of three amino acids namely glutamate, cysteine and glycine (Figure 2.9). The peptide bond between the carboxyl group of the glutamate side chain and the amino group of cysteine is known as the gamma (γ) peptide bond which is slightly different from the normal peptide bonds in proteins. The gamma (γ) carboxyl group links cysteine and glutamate amino acids together. The carboxyl group of the cysteine amino acid in other words forms a peptide bond with the amino group of glycine. GSH is a vital non-protein thiol compound as well as a very essential hydrophilic antioxidant in the cell (Pandey and Rizvi, 2010).

2.5. Biosynthesis of Glutathione

Two important steps are involved in GSH biosynthesis. In the first stage, L-glutamate reacts with L-cysteine with the use of ATP to produce γ -glutamyl cysteine through the action of the γ -glutamyl cysteine synthetase otherwise known as glutamate cysteine ligase (GCL). In the second step, γ -glutamyl cysteine together with L-glycine and ATP undergo a reaction to generate the tripeptide γ -glutamyl-cysteinyl-glycine (GSH) by the action of glutathione synthetase (Figure 2.10) (Espinosa-Diez et al., 2015).

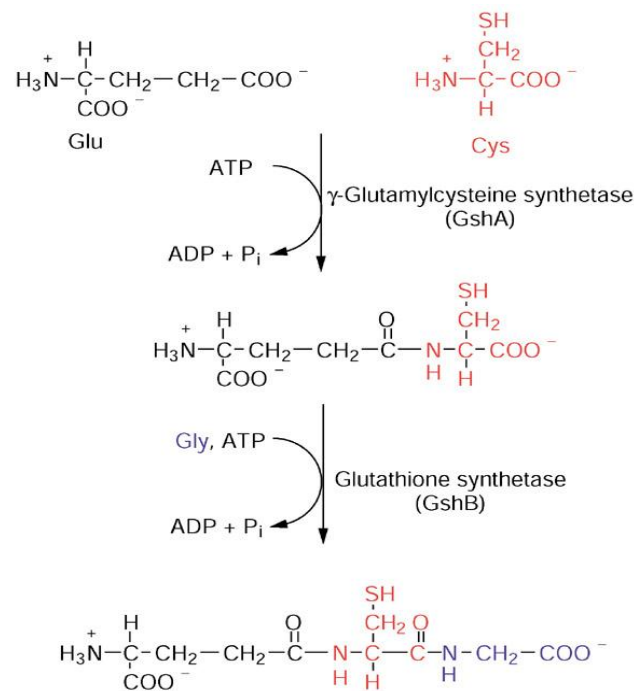


Figure 2.10. Biosynthesis of glutathione (Copley and Dhillon, 2002)

2.6. Functions of Glutathione and Glutathione Reductase

GR and GSH are found in all compartments of the mammalian cells and they play very important roles in the antioxidant defense system. In normal body metabolism, GR maintains GSH/GSSG ratio by converting GSSG to GSH using one mole of NADPH as an electron donor in order to protect cells against damage, but in the case of oxidative stress, GSH/GSSG ratio can be used to determine oxidative stress state of cell. GSH also helps the conversion of inactive antioxidants (vit C & E) to their active forms. Different antioxidant enzymes like GPx and GST use GSH as a cofactor during their actions. GSH plays a significant role in xenobiotic detoxification, acting as a reservoir for cysteine amino acid and also protecting the thiol group of proteins by maintaining them in their reduced forms since their oxidation can cause altered cell structure and function (Pandey and Rizvi, 2010).

Through GR and other antioxidant enzyme action, GSH plays a very important function in nutrient metabolism and regulation of cellular activities like synthesis of DNA and proteins, gene expression, cell growth and death, immune response and protein glutathionylation (Pandey and Rizvi, 2010). It is also able to

correlate different signaling pathways (proapoptotic and antiapoptotic) by protecting them against apoptosis (Masella et al., 2005). Several transcription factors such as AP-1, NF- κ B and SP-1 are activated and controlled by GSH. For instance, the role of GR in the generation of GSH level is very crucial in the enhancement of AP-1 binding (Meyer et al., 1993). Hydrogen peroxide detoxification is carried out by GSH with the help of the antioxidant enzyme GPx (Birben et al., 2012). The membrane lipids are protected from free radical attacks by GSH (Curello et al., 1985). Glutathione system is the most essential endogenous protecting system against oxidative damage in cells (Pandey and Rizvi, 2010). Depletion or inhibition of this antioxidant molecule has been observed in different ailments like cancer and neurodegenerative diseases (Townsend et al., 2003), diabetes (Kalkan and Suher, 2013) sickle cell anemia (Morris et al., 2008), cystic fibrosis (Griese et al., 2013) and AIDS (Wu et al., 2004).

2.7. Antioxidant Mechanism of Reduced Glutathione

During normal aerobic metabolism, harmful oxygen radicals or free radicals are produced. The accumulation of these toxic radicals can lead to cellular modification. The cells are usually in a constant battle to fight against ROS by building up antioxidant defense. GSH protects cells against harmful oxygen species and free radicals. This is due to the nucleophilic nature of the thiol (-SH) group and the high reaction rate between free radicals and the thiol (-SH) group. GSH converts H_2O_2 to H_2O through the action of selenium dependent enzyme, glutathione peroxidase. At this point, GSH is oxidized to its disulphide form (GSSG). Through GR enzyme action, GSSG is reduced back to GSH using NADPH as a reducing factor. Other antioxidant enzymes like catalase produced by peroxisomes can also reduce H_2O_2 to H_2O . Since the mitochondria is the power house of the cell where aerobic action takes place, $\text{O}_2^{\bullet-}$ produced is converted to H_2O_2 by SOD and H_2O_2 is converted to H_2O by glutathione peroxidase because of the absence of catalase in the mitochondria (Figure 2.11) (Mari et al., 2009).

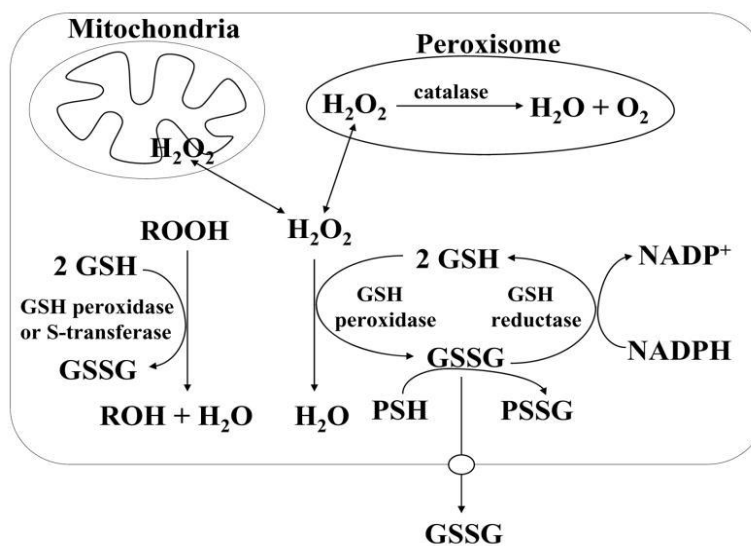


Figure 2.11. Antioxidant mechanism of glutathione (Lu, 2009)

2.8. Reactive Oxygen Species

Reactive oxygen species (ROS) as well as reactive nitrogen species (RNS) correlate to exert both advantageous and damaging effects to the cells in the living system (Pham-Huy et al., 2008). Their beneficial effect is very necessary for protecting cells from harmful substances, they are also very useful in regulatory processes (Luperchio et al., 1996). In a situation where ROS exceeds the system's ability to eliminate them, it can lead to oxidative stress, causing damage to biomolecules and resulting in different health complications (Ismail et al., 2010). ROS exist in different forms namely; hydrogen peroxide (H_2O_2), superoxide anion ($O_2^{\cdot-}$), hydroxyl radical ($\cdot OH$), singlet oxygen (1O_2) etc. (Birben et al., 2012).

2.9. Sources of Reactive Oxygen Species

ROS are produced during normal cellular metabolism particularly by mitochondria during electron transport chain, by uncontrolled stimulation of NADPH oxidase and chiefly from high oxygen consumption (Valko et al., 2007). Certain life style activities (exercise, stress, alcohol consumption, cigarette smoking), environmental pollutants, infection, drug metabolism etc. can also lead to the generation of ROS. It can cause lipid peroxidation and DNA damage eventually lead to the destruction of the macromolecules and in long term necrosis and apoptosis (Figure 2.12) (Tokarz et al., 2013).

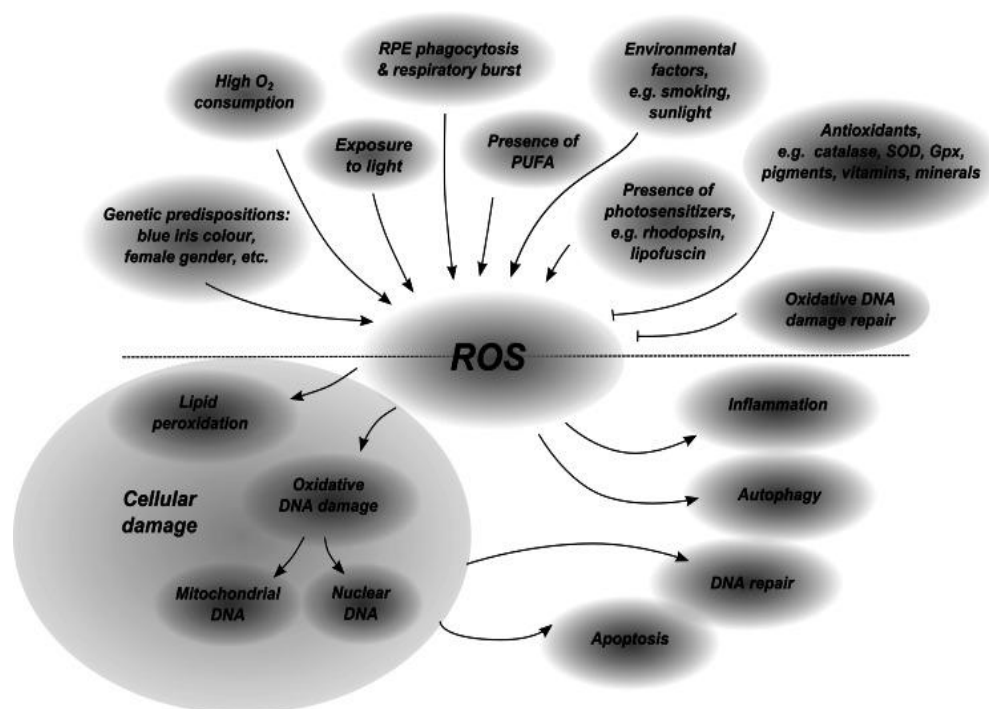


Figure 2.12. Production and effects of ROS (Tokarz et al., 2013)

2.10. Oxidative Stress

Oxidative stress occurs when there is an imbalance between the production of ROS and antioxidants. This can be due to reduction in antioxidant enzymes or accumulation of ROS. Oxidative stress is a concession of aerobic organisms due to their normal aerobic activities. It can be instigated by the internal or external factors. (Djordjevic et al., 2008). Different health complications are attributed to oxidative stress like cardiovascular diseases (Dhalla et al., 2000), neurodegenerative diseases (Kim et al., 2015), cancer (Reuter et al., 2010), diabetes (Giacco and Brownlee, 2010) and hypertension (Harrison and Gongora, 2009). During oxidative stress, the body tries to fight with the free radicals by initializing the expression of genes that encode different antioxidant enzymes. In case, ROS accumulation exceeds the body's ability to fight, it results in damage to the cell structures and functions of important macromolecules (DNA, proteins and lipids), causes apoptosis, inflammation and tissue damage (Figure 2.13) (Lobo et al., 2010).

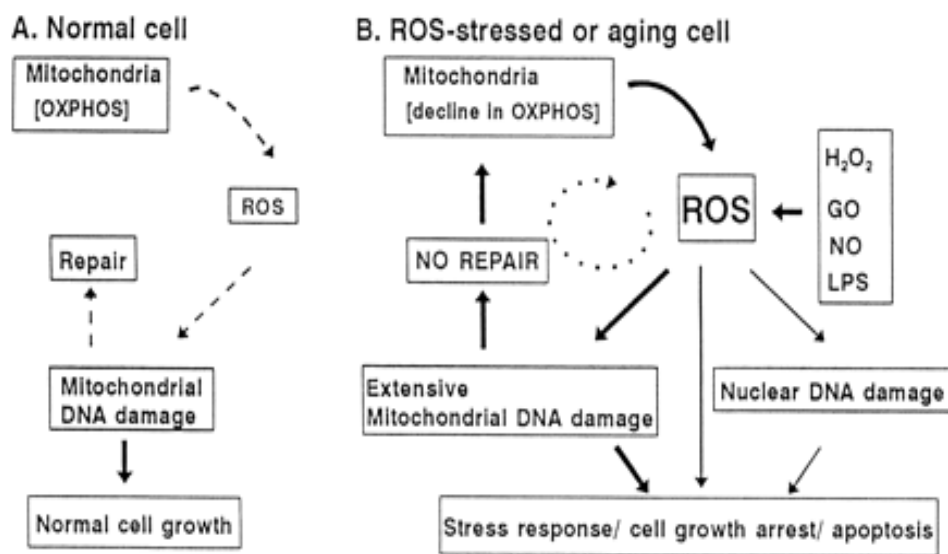


Figure 2.13. Schematic presentation of ROS mechanism and damage (Yakes and Van Houten, 1997)

2.11. The Role of Glutathione Reductase in Oxidative Stress Related Diseases

Different health problems have been linked to cellular damage and alterations in biomolecule structures as a result of accumulation of ROS. Diminished level of GSH is a predominant attribute that instigates apoptosis (Ortega et al., 2011). Apoptosis as a result of oxidative stress has been linked to different health complications like neurodegenerative diseases (Chen et al., 2012), sickle cell anemia (Queiroz and Lima, 2013), amyotrophic lateral sclerosis (Pham-Huy et al., 2008), aging and cystic fibrosis (Galli et al., 2012).

Glutathione reductase also plays a very crucial role in safeguarding the red blood cells (RBC) and other cell membranes by providing GSH. The depletion of this enzyme will expose the RBC and biological cell membranes to oxidative injury thereby resulting in anemia (severe to moderate) against exposure to some chemicals or drugs (Waggiallah and Alzohairy, 2011). Variation in the glutathione concentration and accumulation of glutathione disulphide as a result of GR depletion will lead to ROS accumulation, in a long run, this will result in oxidative stress which is a hallmark for different health complications listed below (Zhao et al., 2009).

Parkinson's disease (PD) is a neurodegenerative cerebrum ailment that influences the nervous system (Kakkar and Dahiya, 2015). This condition emerges gradually and steadily and aggravates with time. Early manifestations of this disease include trembling, stiffness, dullness and difficulty in motion. Parkinson's disease occurs as a result of dopaminergic neuron depletion in the substantia nigra pars compacta (SNPc). Nevertheless, oxidative phosphorylation which occurs in the mitochondria and generation of ROS are known to cause neuronal demise in PD, that is, increased stress as a result ROS production is one of the suggested mechanisms for the depletion of dopaminergic neurons in PD. Hence, mitochondrial complex I is known to be one of the main ROS sources (Subramaniam and Chesselet, 2013). Also, elevation in oxidative harm to biomolecules as a result of decreased GSH/GSSG ratio and its related enzymes has been attributed to PD (Beal, 1995). Glutathione is very crucial in the brain for defense against free radicals and depletion of glutathione in the brain will result in oxidative damage which is a very common pathogenesis among patients with PD (Aoyama and Nakaki, 2013; Dias et al., 2013). GR is a known essential enzyme in GSH production in the brain and impairment of the GSH molecule only explains GR enzyme disruption (Barker et al., 1996).

Sickle cell anemia (SCA) is simply an erythrocyte disorder. It is a life threatening ailment correlated with the inability of hemoglobin to transport oxygen throughout the body (Kawadler et al., 2015). SCA is an autosomal recessive ailment caused by displacement of two amino acids in the β -chain of the hemoglobin molecule. Glutamic acid found in the 6th position of the β -chain is replaced with valine (Queiroz and Lima, 2013). This defect further results in a crescent shaped hemoglobin making it inactive in oxygen transport (Enwonwu, 1988). Apart from the fact that SCA is a hereditary disease, it is also important to know the effect of GR activity in patients with SCA. It is well known that accumulation of ROS is very conversant among patients with sickle cell anemia. The mechanism in which oxygen radicals are generated is 1.7 times higher in sickle-cell RBC, making these cells defenseless against oxidative stress (Henneberg et al., 2013). In SCA, GSH/GSSG level is decreased as a result of GR depletion (Nur et al., 2011).

2.12. Fluoxetine

Fluoxetine (N-methyl-3-phenyl-3-[4-(trifluoromethyl)phenoxy]propan-1-amine) is widely known as the trade name Prozac. It is a commonly used antidepressant medication in the treatment of depression which is very common in patients with psychological disorders. Fluoxetine is known to carry out its action as a selective serotonin re-uptake inhibitor (SSRI) by blocking serotonin transporter (Kullyev et al., 2010; Sawyer and Howell, 2011). Apart from depression, fluoxetine is also used in the treatment of anxiety disorders (Birmaher et al., 2003), obsessive compulsive disorder (OCD) (Farnam et al., 2008), premenstrual disorder (Rossi et al., 2004), post-traumatic stress disorder and borderline personality disorder (Salzman et al., 1995; Coccaro and Kavoussi, 1997; Xu et al., 2011). It is taken orally and widely distributed in all tissues with highest concentrations in the lungs and liver. High fluoxetine concentration in these tissues is related to the fact that these tissues are rich in lysosomes (Daniel and Wojcikowski, 1997).

After oral intake, the antidepressant is known to be metabolized in the liver to its active form desmethyl metabolite norfluoxetine (Johnson et al., 2007). Just like other medications, fluoxetine causes different side effects like sleep interference, nausea, sexual deterioration, headaches, changes in appetite and dry mouth (Ferguson, 2001). Long term use of this SSRI has been linked to increased risk of diabetes (Anderson et al., 2009; Isaac et al., 2013).

The SSRI is a racemic mixture of R-fluoxetine and S-fluoxetine enantiomers, the same is applicable to its desmethyl metabolite norfluoxetine (Figure 2.14). During metabolism, the S-fluoxetine is converted to S-norfluoxetine and the R-fluoxetine is converted to R-norfluoxetine. When comparing the enantiomers of fluoxetine, the S-form is known to be 5 times stronger than the R-form, as for the enantiomers of norfluoxetine, the S-form is known to be 20 times stronger than the R-form (Scordo et al., 2005).

During fluoxetine metabolism, the ability of fluoxetine to be effectively metabolized to norfluoxetine relies on the cytochrome p450 (CYP) isozymes (CYP2D6, CYP2C9, and to a lesser extent CYP2C19). These isozymes are responsible for the demethylation of fluoxetine to norfluoxetine. However, the S-form of fluoxetine and norfluoxetine are known as the strong inhibitors of CYP2D6

than their R-forms, making it possible for fluoxetine action to take effect especially in individuals with fast metabolizing system (Fjordside et al., 1999; Ring et al., 2001). After fluoxetine administration, the half-life for norfluoxetine in human tissues is 7-15 days and that of fluoxetine is 1-4 days (Sawyer and Howell, 2011).

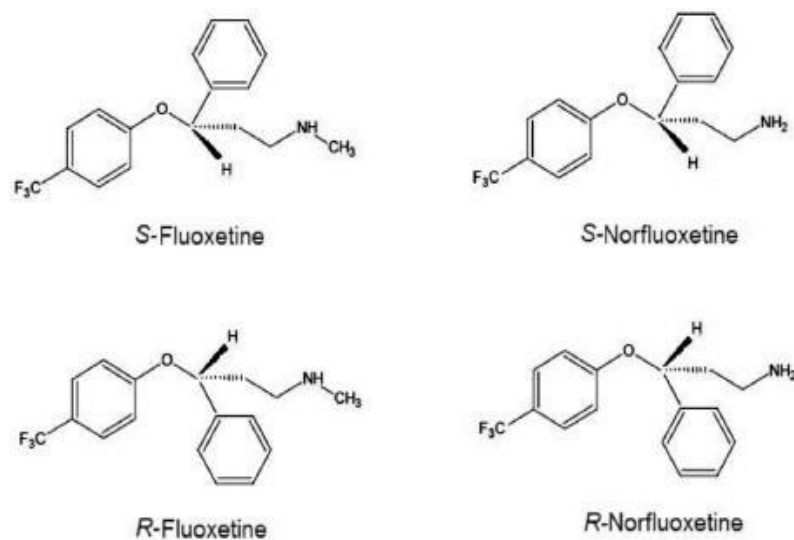


Figure 2.14. Structures of fluoxetine and norfluoxetine enantiomers (Jordana et al., 2011).

3. MATERIALS AND METHODS

3.1. Chemicals

Fluoxetine hydrochloride was procured from LKT Laboratories (St. Paul, MN, USA). Acetic acid was acquired from Riedel-de Haën (Germany). Orthophosphoric acid was obtained from Applichem (Darmstadt, Germany). Coomassie Brilliant Blue G-250 and Coomassie Brilliant Blue R-250 were purchased from Fluka Analytical (United Kingdom). Oxidized glutathione was obtained from Fluka Analytical (Switzerland). Roti-Mark protein standard was obtained from Carl Roth GmbH (Karlsruhe, Germany); 2,6-dichlorophenol indophenol was provided from BDH Chemicals (United Kingdom). Potassium phosphate (monobasic and dibasic), glycine, ethanol, methanol, sodium azide, acrylamide, N, N'-methylenebisacrylamide, ammonium persulfate, dimethyl sulphoxide (DMSO), N, N, N', N'-tetramethylenediamine, silver nitrate, formaldehyde, 2-mercaptoethanol, Trizma base, sodium dodecyl sulfate, sodium carbonate, sodium thiosulfate, glycerol, bovine serum albumin, bromophenol blue and reduced nicotinamide adenine dinucleotide phosphate (NADPH), glutathione reductase purified from baker's yeast, thiazolyl blue tetrazolium bromide (MTT) were obtained from Sigma Aldrich (St. Louis, MO, USA).

3.2. Methods

3.2.1. Preparation of the Glutathione Reductase

Glutathione reductase (GR) purified from baker's yeast was purchased from Sigma Aldrich (St. Louis, MO, USA) as a suspension in 3.6 M ammonium sulfate containing 0.1 M dithiothreitol. In order to remove ammonium sulfate, enzyme was centrifuged at 20800 xg for 20 minutes at 4°C. The supernatant was removed and the pellet was dissolved in 20 mM phosphate buffer pH 7.4.

3.2.2. Determination of the Protein Concentration

Concentration of GR, purified from baker's yeast was determined according to Bradford protein assay (Bradford, 1976). Bradford assay is a popular method used for the determination of the protein concentration owing to the fact that it is rapid, sensitive and relatively specific (Aminian et al., 2013). Coomassie Brilliant Blue G-

250 (CBB) was used in Bradford protein assay. The acidic dye CBB is the most commonly used for determination of proteins because the method is simple, rapid and straightforward (Grintzalis et al., 2015). It binds precisely to positively charged proteins. After binding, the absorbance wavelength shifts from 470 nm to 595 nm. The absorbance of the dye-protein complex is measured at 595 nm and the protein concentration is determined by using bovine serum albumin standard prepared in parallel.

Preparation of the Bradford reagent: 25 mg of Coomassie Brilliant Blue G-250 was weighed and dissolved in 12.5 ml of absolute ethanol and 25 ml of 85% orthophosphoric acid was added and the final volume was adjusted to 250 ml with distilled water. The mixture was filtered by using Whatman No: 1 filter paper and stored in a dark bottle at room temperature.

Bovine serum albumin (BSA) was used as a standard. Stock BSA (1 mg/ml) solution was prepared, it was then diluted to obtain six standard solutions (50 µg/ml, 100 µg/ml, 200 µg/ml, 300 µg/ml, 400 µg/ml and 500 µg/ml). Standard BSA solutions and samples (20µl) were mixed with 1 ml of Bradford reagent and placed in dark for 5 mins. Then, the absorbances of standards and samples were measured at 595 nm by using Lambda 25 UV/VIS Spectrophotometer (Perkin Elmer, Singapore). The standards and samples were prepared in triplicates. Concentration of GR was determined from the standard curve depicted A_{595} versus BSA concentrations.

3.2.3. Native-Polyacrylamide Gel Electrophoresis (Native-PAGE)

In determining the purity of GR enzyme, discontinuous native page was used (Hames, 1998). The protein bands were visualized through the use of Coomassie Brilliant Blue R-250, silver and activity stainings. The concentrations of separating and stacking gels used in the CBB and silver stainings were 6% and 4%, respectively. The gel prepared for activity staining was made up of 10% separating and 4% stacking gels for decreasing the diffusion of enzymatic product.

Stock Reagents for Discontinuous Native-PAGE

- 30% Acrylamide/Bisacrylamide solution (29.4% acrylamide/0.6% N,N-methylenebisacrylamide)
- Separating gel buffer: 1.5 M Tris/HCl, pH 8.8
- Stacking gel buffer: 0.5 M Tris/HCl, pH 6.8
- 10x Electrode (running) buffer: 25 mM Tris (Base), 192 mM glycine
- 2x Sample buffer: 10 mg bromophenol blue was dissolved in 1.25 ml of 0.5 M Tris/HCl, pH 6.8 containing 4 ml glycerol,. The volume was adjusted to 10 ml with distilled water.
- 10% ammonium persulfate (APS), prepared daily.
- N,N,N,'N'-tetramethylethylenediamine (TEMED)

Table 3.1. Volumes used in gel preparation of Native-PAGE

	Separating Gel		Stacking Gel (4%)
	6%	10%	
30% Acrylamide/Bisacrylamide (ml)	3	5	1.33
1.5 M Tris/HCl, pH 8.8 (ml)	3.75	3.75	-
0.5 M Tris/HCl, pH 6.8 (ml)	-	-	2.5
Distilled water (ml)	8.25	6.17	6.12
10% APS (μ l)	75	75	40
TEMED (μ l)	7.5	7.5	10
Total Volume (ml)	15	15	10

Preparation of Gel for Native-PAGE

1.5 mm spacers were used for the gel preparation. The spacer and the plain glasses were placed vertically on the casting stand. After gel preparation (Table 3.1), 6.5 ml of the separating gel mixture was dispensed into the plain glasses and distilled water was layered on in order to have a smooth surface, then it was left for about 1 hour for polymerization. After polymerization of the separating gel, water is discarded. Stacking gel mixture (Table 3.1) was added onto the polymerized separating gel and the 10 well comb was immediately placed in the gel and then it was kept for about 1

hour 30 minutes for polymerization. The gel prepared was removed from the casting stand and placed in the electrophoresis assembly and transferred into the electrophoresis tank. Tank was filled with running buffer and the 10 well comb was removed. Wells were washed with the running buffer solution before loading the samples.

Sample Preparation for Native-PAGE

Sample preparation was carried out in three different ways according to the staining methods employed. First of all 2-mercaptoethanol was diluted 1:100 and 1.13 μl of it was added to 15 μl of stock enzyme and incubated for 1 hour at room temperature. Final enzyme concentration in each well was adjusted to 5 μg , 3.75 μg , 2.5 μg and 1.25 μg for CBB staining; 0.5 μg , 0.375 μg , 0.25 μg and 0.125 μg for silver staining and 4 μg , 8 μg and 12 μg for activity staining.

- Sample preparation for CBB staining

1. 1 μl of stock enzyme + 3.8 μl of 20 mM phosphate buffer pH 7.4
2. 1 μl of stock enzyme + 5.4 μl of 20 mM phosphate buffer pH 7.4
3. 1 μl of stock enzyme + 8.6 μl of 20 mM phosphate buffer pH 7.4
4. 1 μl of stock enzyme + 18.2 μl of 20 mM phosphate buffer pH 7.4

Just before the application of the sample into the gel, sample was mixed with sample loading buffer at 1:1 ratio and 20 μl of the sample was loaded into the wells.

- Sample preparation for silver staining

First of all enzyme was diluted at 1:10 ratio.

1. 4 μl of diluted enzyme + 15.2 μl 20 mM phosphate buffer pH 7.4
2. 3 μl of diluted enzyme + 16.2 μl 20 mM phosphate buffer pH 7.4
3. 2 μl of diluted enzyme + 17.2 μl 20 mM phosphate buffer pH 7.4
4. 1 μl of diluted enzyme + 18.2 μl 20 mM phosphate buffer pH 7.4

Just before the application of the sample into the gel, sample was mixed with sample loading buffer at 1:1 ratio and 20 μl of the sample was loaded into the wells.

- **Sample preparation for activity staining**

1. 10 μ l of stock enzyme + 20 μ l dH₂O + 10 μ l sample loading buffer
 2. 20 μ l of stock enzyme + 10 μ l dH₂O + 10 μ l sample loading buffer
 2. 30 μ l of stock enzyme + 10 μ l sample loading buffer
- 20 μ l of sample was loaded into the wells.

Bio-Rad Miniprotean Tetra Cell electrophoresis system was used. Electrophoresis was initiated with 120 V and when the samples migrated into the separating gel, the voltage was increased to 150 V. Electrophoresis was completed when the bromophenol blue dye reached about 1 cm to the end of the gel. Gels were transferred into petri dishes for staining processes.

3.2.4. Sodium Dodecyl Sulfate-Polyacrylamide Gel Electrophoresis (SDS-PAGE)

SDS-PAGE was used to determine the purity of the enzyme and also its relative molecular weight. Concentrations of separating and stacking gels were 7% and 4%, respectively (Laemmli, 1970).

Stock Reagents for Discontinuous SDS-PAGE

- 30% Acrylamide/Bisacrylamide solution (29.4% acrylamide/0.6% N,N-methylenebisacrylamide)
- Separating gel buffer: 1.5 M Tris/HCl, pH 8.8
- Stacking gel buffer: 0.5 M Tris/HCl, pH 6.8
- 5x Electrode (running) buffer pH 8.3 was taken from already prepared native gel running buffer (10x) containing 15 g/L Tris Base and 72 g/L glycine. To the 5x electrode buffer, 6 gr of SDS was added.
- 2x Sample buffer: 3 ml of 1.5 M Tris/HCl pH 6.8, 5 gr glycerol i.e 4 ml, 1.6 ml of BPB, 2.8 μ l of β -ME (added immediately during sample preparation), 0.37 ml of dH₂O, 1 ml of 10% SDS
- 10% SDS solution
- 10% ammonium persulfate (APS), prepared daily
- N, N, N,'N'-tetramethylethylenediamine (TEMED)

Preparation of Gel for SDS-PAGE

1.5 mm spacers were used for the gel preparation. The spacer and the plain glasses were placed vertically on the casting stand. After gel preparation (Table 3.2), 6.5 ml of the separating gel mixture was dispensed into the plain glasses and distilled water was layered on in order to have a smooth surface, then it was left for about 1 hour for polymerization to occur. After polymerization of the separating gel, water was discarded. Stacking gel mixture (Table 3.2) was added onto the polymerized separating gel and the 10 well comb was immediately placed in the gel and kept for about 1 hour 30 minutes for polymerization. The plain glasses were removed from the casting stand and placed in the electrophoresis assembly and transferred into the electrophoresis tank. Tank was filled with running buffer containing SDS and the 10 well comb was removed. Wells were washed with the running buffer solution before loading the samples.

Table 3.2. Volumes Used in Gel Preparation of SDS-PAGE

	Separating Gel (7%)	Stacking gel (4%)
30% Acrylamide/Bisacrylamide (ml)	3.5	1.33
1.5 M Tris/HCl, pH 8.8 (ml)	3.75	-
0.5 M Tris/HCl, pH 6.8 (ml)	-	2.5
Distilled water (ml)	7.57	6.07
10% SDS (μ l)	100	100
10% APS (μ l)	75	50
TEMED (μ l)	7.5	10
Total Volume	15	10

Sample Preparation for SDS-PAGE

Sample preparation was carried out in two different ways according to the staining methods employed. Final enzyme concentration in each well was adjusted to 4 μ g, 8 μ g and 12 μ g for CBB staining; 0.4 μ g, 0.8 μ g and 1.2 μ g for silver staining. For relative molecular weight estimation (Mr), roti-mark protein molecular weight marker was used.

- **Sample preparation for CBB staining**

1. 10 µl of stock enzyme + 20 µl of dH₂O + 10 µl of sample loading buffer
2. 20 µl of stock enzyme + 10 µl of dH₂O + 10 µl of sample loading buffer
3. 30 µl of stock enzyme + 10 µl of sample loading buffer

Samples were incubated at 95°C for 3 min and after cooling to room temperature, 20 µl of sample was loaded into the wells.

- **Sample preparation for silver staining**

1. 1 µl of stock enzyme + 29 µl of dH₂O + 10 µl of sample loading buffer
2. 2 µl of stock enzyme + 28 µl of dH₂O + 10 µl of sample loading buffer
3. 3 µl of stock enzyme + 27 µl of dH₂O + 10 µl of sample loading buffer

Samples were incubated at 95°C for 3 min and after cooling to room temperature, 20 µl of sample was loaded into the wells.

Bio-Rad Miniprotein Tetra Cell electrophoresis system was used. Electrophoresis was initiated with 150 V and when the samples migrated into the separating gel, the voltage was increased to 200 V. Electrophoresis was completed when the bromophenol blue dye reaches about 1 cm to the end of the gel. Gels were transferred into petri dishes for staining processes.

3.2.5. Coomassie Brilliant Blue (CBB) R-250 Staining

After native and SDS-PAGE, CBB staining protocol was carried out in order to visualize the protein bands on the gel. Staining solution was made up of 0.1% Coomassie Brilliant Blue R-250, 40% methanol and 10% acetic acid. After electrophoresis, gel was stained with the solution for 30 minutes and then transferred into destaining solution. The destaining solution was made up of 40% methanol and 10% acetic acid. Destaining solution was replaced till the background of the gel was clear. Following destaining process, gel was stored in 5% acetic acid at 4°C (Wilson, 1979).

3.2.6. Silver Staining

Silver staining was also carried out in order for a better visualization of the protein bands. After native and SDS-PAGE procedures were completed, gels were stained with silver nitrate according to the method of Blum et al. with slight modifications (Blum et al., 1987). Gels were fixed with 50% methanol, 12% glacial acetic acid and 0.005% formalin solution for 2 hours. After fixation, gels were washed three times with 50% ethanol for 20 minutes. Gels were sensitized with 0.02% sodium thiosulfate for 2 minutes and then washed with distilled water three times for 20 seconds. Then the gels were stained with 0.2 % silver nitrate and 0.076% formalin solution for 20 minutes. After staining, gels were washed with distilled water twice for 20 seconds. The stained gels were kept in 6% sodium carbonate, 0.05 formalin and 0.0004% sodium thiosulfate solution until the bands were visible. When the bands were clearly seen, gels were washed with distilled water twice for 2 minutes. Staining was terminated by the addition of a stop solution which was made up of 40% methanol and 10% glacial acetic acid and gels were placed in this solution for 20 minutes. After completion of the staining procedure, gels were stored in 1% glacial acetic acid solution at 4°C.

3.2.7. Activity Staining

On the completion of native-PAGE procedure, the activity staining method of Graubaum for cellulose acetate was adapted to gels as described below (Graubaum, 1981). Gels were incubated in three different solutions. First, gel was incubated in 15 ml of 100 mM potassium phosphate buffer pH 7.5 for 2 minutes for buffer exchange. Then, gel was transferred into 15 ml of 100 mM potassium phosphate buffer pH 7.5 containing 1.0 mg MTT and 0.100 mg of dichlorophenol indophenol for 10 minutes then the solution was discarded. Finally, gel was incubated in the 15 ml of 100 mM potassium phosphate buffer pH 7.5 containing 2.5 mg NADPH and 18 mg GSSG. Gel was placed in this solution until color developed.

3.2.8. Measurement of Glutathione Reductase Enzyme Activity

Glutathione reductase enzyme activity was carried out according to Carlberg and Mannervik's method through the use of Perkin Elmer Lambda 25 UV/VIS

Spectrophotometer (Carlberg and Mannervik, 1975). GR activity was measured in 100 mM potassium phosphate buffer pH 7.4, containing 1 mM GSSG, 0.1 mM NADPH and 25 μ l of enzyme. The enzyme GR was added lastly in order to initiate the reaction. Decrease in the absorbance at 340 nm was monitored for 30 seconds at 37°C. In general, each activity measurement was repeated three times. Average activity (U/L) values were converted to specific activity (U/mg protein) and the calculated specific activity values were used to draw the following plots: Optimum pH, optimum temperature, Michaelis-Menten, Lineweaver-Burk and Dixon plots (Segel, 1975).

$$\text{Specific Activity (Unit/mg protein)} = \frac{\Delta\text{Abs}_{340} \times V_t \times 1000}{6.22 \times V_s \times [\text{Protein}]}$$

$\Delta\text{Abs}_{340}/\text{min}$: Absorbance change per minute at 340 nm

V_t : Volume of total activity mixture (500 μ l)

V_s : Sample volume (μ l) used to measure enzyme activity

6.22 : Extinction coefficient of NADPH (mM)

1000 : A factor used to convert ml to liter

Kinetic parameters ($K_{m\text{GSSG}}$, $V_{m\text{GSSG}}$ and $K_{m\text{NADPH}}$, $V_{m\text{NADPH}}$) for glutathione reductase enzyme were determined by using different concentrations of GSSG (0.05 mM, 0.1 mM, 0.25 mM, 0.5 mM, 1 mM, 1.5 mM and 2 mM) while keeping the NADPH concentration constant (0.1 mM) and also by using different concentrations of NADPH (0.01 mM, 0.015 mM, 0.02 mM, 0.04 mM and 0.1 mM) while keeping GSSG concentration constant (1 mM).

3.2.9. Determination of Optimum pH

For the determination of optimum pH of the GR, the reaction mixtures were made up four different concentrations of potassium phosphate buffer (50 mM, 100 mM, 150 mM, 200 mM) for different pH values (6, 6.5, 7, 7.5, 8, 8.5, 9). The activity of GR was measured in buffers prepared at different pH and concentration by using 1 mM GSSG, 0.1 mM NADPH and 25 μ l of GR enzyme. Each pH value and buffer concentration was tested three times at 37°C and the reaction was followed at 340

nm for 30 seconds (Carlberg and Mannervik, 1975). First, the $\Delta A/\text{min}$ vs [buffer] plot was depicted to find the $\Delta A/\text{min}$ at zero buffer concentration by extrapolation. Then $\Delta A/\text{min}$ at zero buffer concentration vs pH graph was plotted to find the optimum pH (Landqvist, 1955).

3.2.10. Determination of Optimum Temperature

GR enzyme activity was measured at different temperatures in order to determine the optimum temperature (Segel, 1975). The reaction was followed at 340 nm for 30 seconds. Reaction mixture comprised of 100 mM potassium phosphate buffer pH 7.5, 1 mM GSSG, 0.1 mM NADPH and 25 μl of glutathione reductase enzyme. Temperature of each reaction medium (20°C, 25°C, 30°C, 35°C, 40°C, 45°C, 50°C, 55°C, 60°C, 65°C, and 70°C) was controlled by using a water bath adjusted to desired temperature. Each measurement was repeated three times. Average specific activity was calculated and used to draw temperature optimum and energy of activation plots (Segel, 1975).

3.2.11. Effect of Fluoxetine on Glutathione Reductase Enzyme Activity

The antidepressant fluoxetine was dissolved in dimethyl sulphoxide (DMSO) at a concentration of 25 mM. Enzyme activity was measured at 340 nm for 30 seconds at 37°C (Carlberg and Mannervik, 1975). Reaction mixture comprised of 100 mM potassium phosphate buffer pH 7.5, 1 mM GSSG, 0.1 mM NADPH, 25 μl of GR and 10 μl of fluoxetine prepared at different concentrations. The final concentrations of fluoxetine used in the reaction medium were 0.05 mM, 0.1 mM, 0.15 mM, 0.2 mM, 0.25 mM, 0.3 mM, 0.35 mM, 0.4 mM, 0.45 mM and 0.5 mM. Each activity measurement was repeated three times for each concentration. Average specific activity was calculated and used to draw graphics.

3.2.12. Inhibitory Kinetic Experiments with Fluoxetine

Kinetic studies for fluoxetine inhibition were carried out to determine K_m and V_m values for GR in the presence of fluoxetine. Fluoxetine was prepared in four different concentrations (0.05 mM, 0.1 mM, 0.2 mM and 0.4 mM) while GSSG (0.0625 mM, 0.125 mM, 0.25 mM, 0.5 mM and 1mM) and NADPH (0.01 mM,

0.015 mM, 0.02 mM, 0.04 mM and 0.1 mM) were prepared in five different concentrations. When fluoxetine and GSSG concentrations were tested, NADPH concentration was kept constant (0.1 mM). Also, when fluoxetine and NADPH concentrations were tested, GSSG concentration was kept constant (1 mM). Each measurement was repeated three times. Decrease in absorbance at 340 nm was followed for 30 seconds at 37°C (Carlberg and Mannervik, 1975). Average specific activity was calculated and used to draw graphics.

3.2.13. Statistical Analysis

SPSS version 22 was used in the estimation of inhibition type and calculation of kinetic parameters.

4. RESULTS

4.1. Determination of the Protein Concentration

Glutathione reductase enzyme purified from baker's yeast was obtained from Sigma Aldrich and used for all experiments. Basically, protein content of the purchased enzyme was determined through the use of Bradford assay (Bradford, 1976). Bovine serum albumin (BSA) standards were prepared at final concentrations of 50 μg , 100 μg , 200 μg , 300 μg , 400 μg and 500 μg . Standard BSA and enzyme sample (20 μl) were mixed with Bradford reagent (1 ml) and incubated for 5 minutes in dark. Absorbances were measured at 595 nm. Glutathione reductase concentration was calculated by using calibration curve (Figure 4.1) and found to be 813 $\mu\text{g/ml}$.

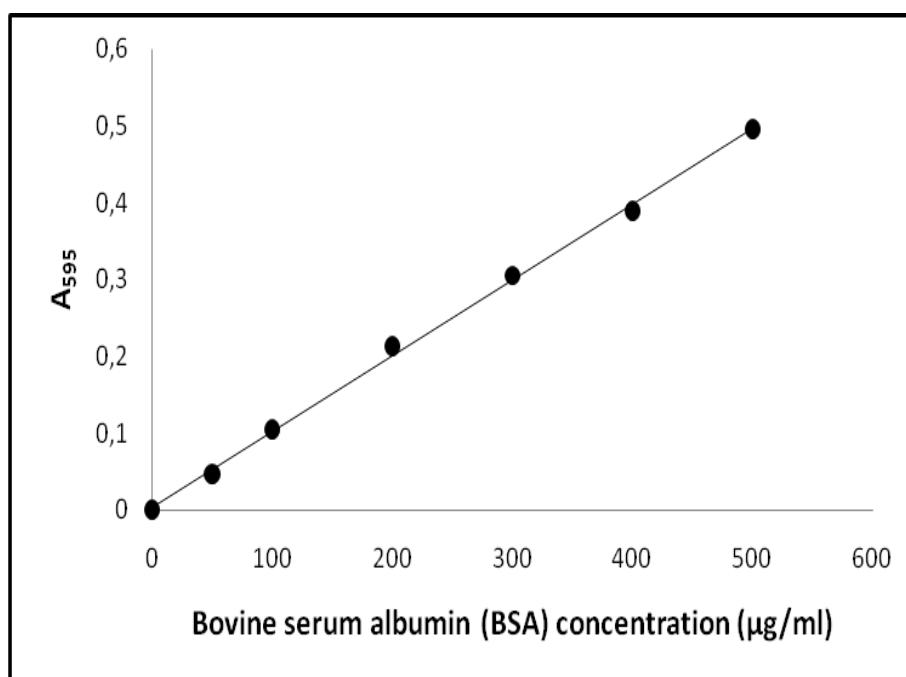


Figure 4.1. Determination of the enzyme concentration by Bradford assay

4.2. Characterization of Glutathione Reductase Enzyme

4.2.1. Purity Control of Glutathione Reductase Enzyme

Native polyacrylamide gel electrophoresis (Native-PAGE) (Figure 4.2 and 4.3) and sodium dodecyl sulfate polyacrylamide gel electrophoresis (SDS-PAGE) (Figure 4.4 and 4.5) were both carried out to justify the purity of the enzyme. Different staining methods like Coomassie Brilliant Blue R-250, activity and silver

stainings were employed to visualize the protein bands. On both gels single protein band was observed to prove the purity of the enzyme (Figure 4.2, 4.3, 4.4 and 4.5.A).

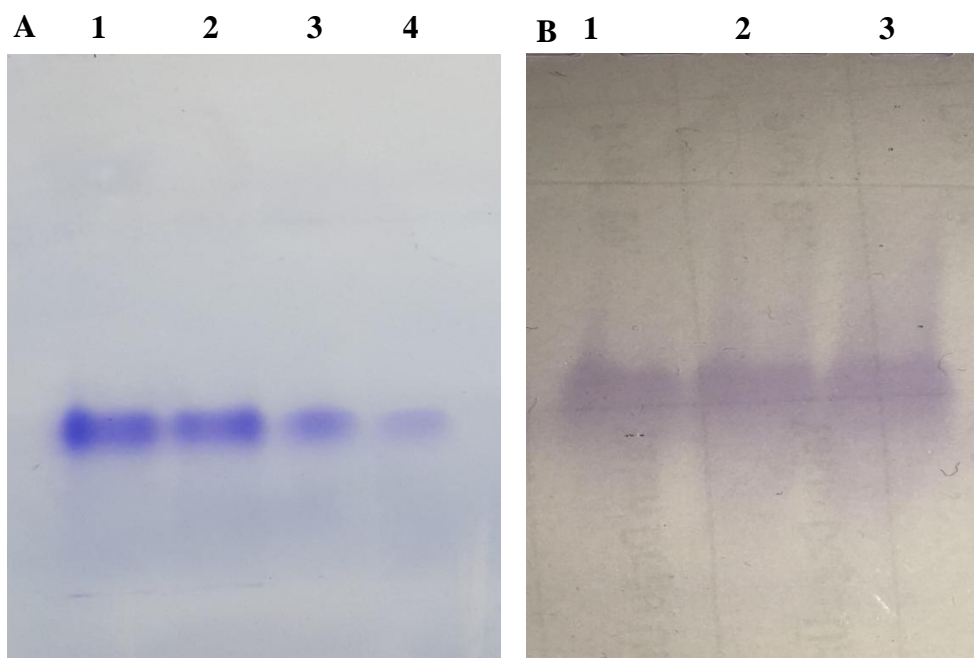


Figure 4.2. Glutathione reductase enzyme on discontinuous native-PAGE. A. Coomassie Brilliant Blue R-250 staining of glutathione reductase. Separating and stacking gels were prepared 6% and 4%, respectively. Protein concentration in lane 1, 5 μg ; lane 2, 3.75 μg ; lane 3, 2.5 μg ; lane 4, 1.25 μg . B. Activity staining of glutathione reductase. Separating and stacking gels were prepared 10% and 4%, respectively. Protein concentration in lane 1, 4 μg ; lane 2, 8 μg ; lane 3, 12 μg .

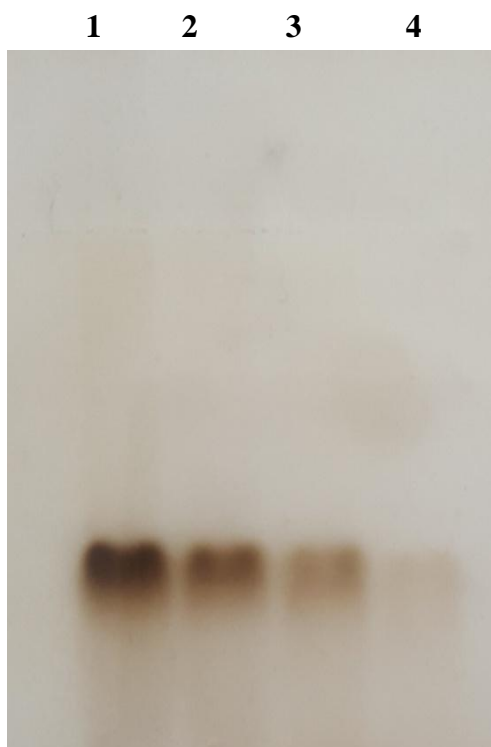


Figure 4.3. Silver staining of glutathione reductase on native-PAGE. Separating and stacking gels were prepared 6% and 4%, respectively. Protein concentration in lane 1, 0.5 μg ; lane 2, 0.375 μg ; lane 3, 0.25 μg ; lane 4, 0.125 μg .

SDS-PAGE was carried out to determine the molecular weight of GR enzyme subunits. After migration, enzyme bands were properly visualized through the use of Coomassie Brilliant Blue R-250 (Figure 4.4) and silver (Figure 4.5.A) stainings. GR is a homodimeric enzyme and subunit molecular weight was calculated as 49 kDa (Figure 4.4.B).

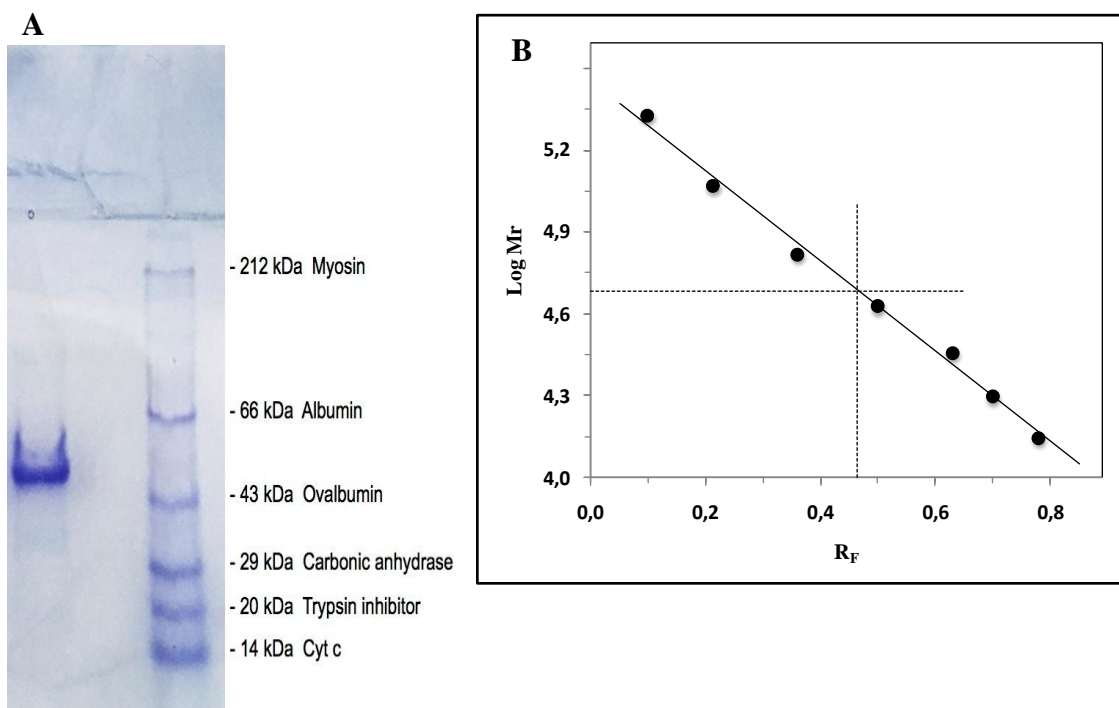


Figure 4.4.A. Visualization of GR enzyme on discontinuous SDS-PAGE by the use of Coomassie Brilliant Blue R-250 staining. Separating and stacking gel were prepared in 7% and 4% respectively. Glutathione reductase enzyme concentration was 4 μ g. Figure 4.4.B. shows Log (Mr) vs R_f plot.

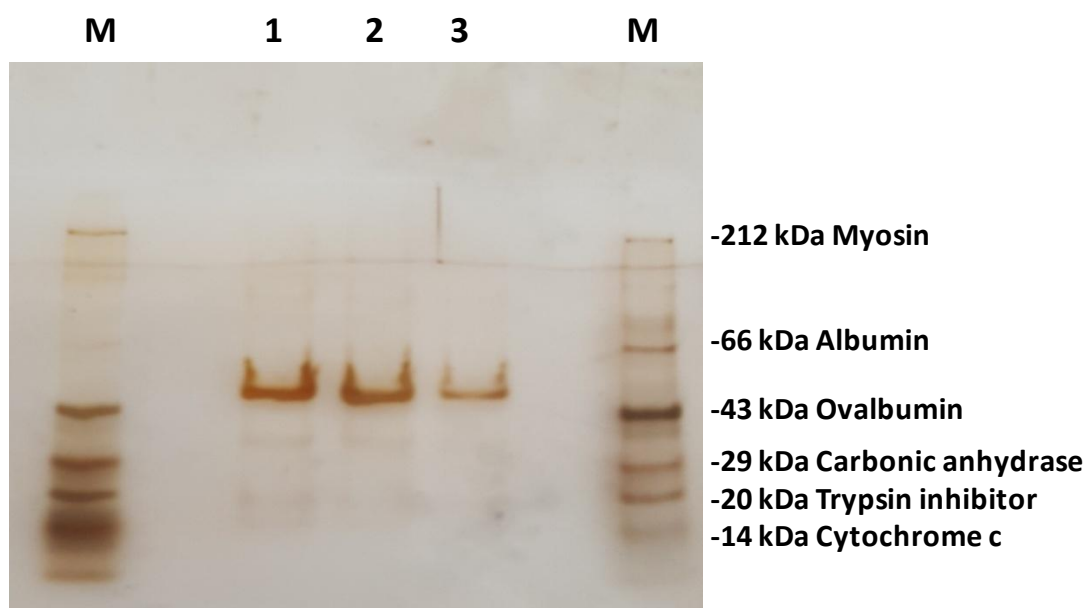


Figure 4.5. Visualization of GR enzyme on discontinuous SDS-PAGE by the use of silver staining. Separating and stacking gel were prepared in 7% and 4% respectively. Glutathione reductase enzyme concentrations in lane 1, 1.2 μg ; lane 2, 0.8 μg ; lane 3, 0.4 μg .

4.2.2. Zero Buffer Extrapolation and Determination of pH Optimum

In order to eliminate the effects of buffer on the optimum pH of the GR, “zero buffer extrapolation” was performed (Landqvist, 1955). This activity measurement was carried out using phosphate buffer at different concentrations (50 mM, 100 mM, 150 mM and 200 mM) and at different pH values (6, 6.5, 7, 7.5, 8, 8.5 and 9). A graph of activity versus buffer concentration was plotted (Figure 4.6) and the activities at zero buffer concentration was determined by extrapolation. Then, a second graph was plotted using the activities at zero buffer concentration versus pH (Figure 4.7) and the optimum pH for GR enzyme was found to be 7.65. Enzyme activity for each pH value and concentration was measured in triplicates and monitored for 30 seconds at 37°C (Carlberg and Mannervick, 1975).

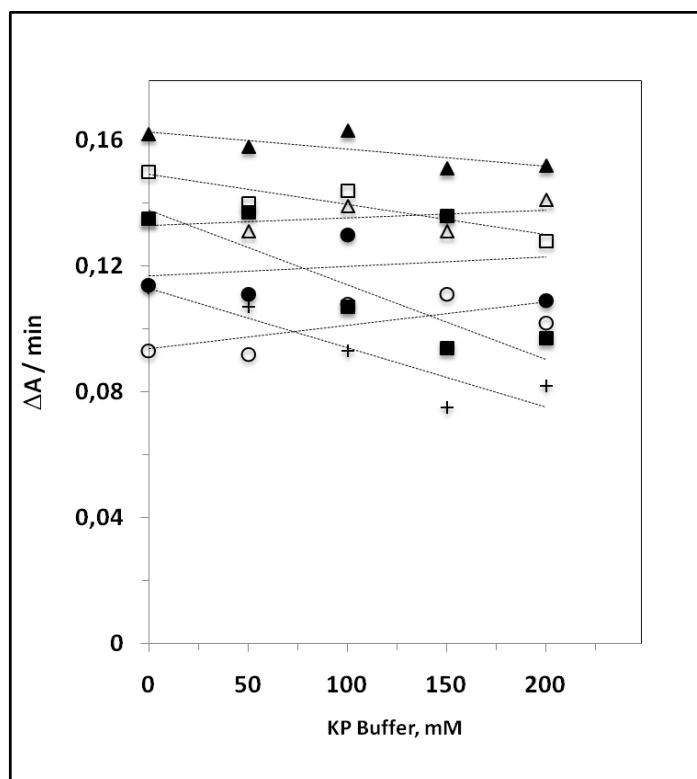


Figure 4.6. $\Delta A/\text{min}$ vs buffer concentration. pH values: 6 (○), 6.5 (●), 7 (Δ), 7.5 (▲), 8 (□), 8.5 (■), 9 (+)

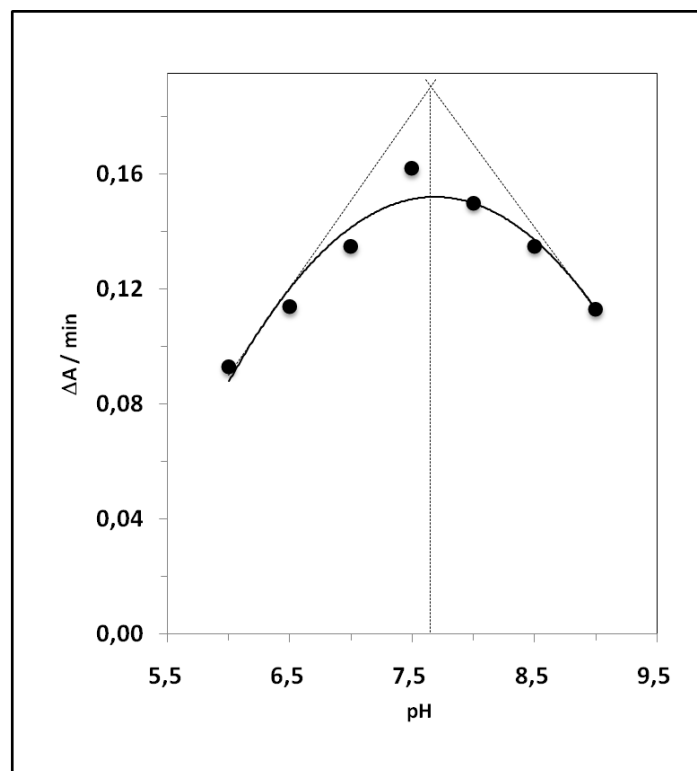


Figure 4.7. $\Delta A/\text{min}$ vs. pH plot

4.2.3. Determination of Optimum Temperature

For the determination of the optimum temperature of GR, the enzyme activity was measured in the reaction medium at different temperatures (20°C, 25°C, 30°C, 35°C, 37°C, 40°C, 45°C, 50°C, 55°C, 60°C, 65°C, and 70°C). Each activity measurement was repeated three times and specific activity (U/mg protein) at each temperature was calculated. A graph of specific activity (U/mg protein) versus temperature (°C) was plotted (Figure 4.8.A) and the optimum temperature was discovered to be 57°C. To determine the activation energy of GR, the logarithms of specific activities versus reciprocal of temperatures in Kelvin was also plotted (Figure 4.8.B). Energy of activation (E_a) and Q_{10} were calculated as 3,544 calories and 1.26, respectively. For E_a and Q_{10} calculations below equations were used:

$$-\text{Slope} = -E_a/2.3R$$

E_a : Activation energy

R : Gas constant

$$E_a = 2.3R T_1 T_2 \log Q_{10}/10$$

Q_{10} : Temperature coefficient

T_1 and T_2 temperatures in Kelvin

4.3. Substrate Kinetics

Kinetic parameters for GR were determined by using different concentrations of GSSG (0.05 mM, 0.1 mM, 0.25 mM, 0.5 mM, 1 mM, 1.5 mM and 2 mM) while keeping the NADPH concentration constant (0.1mM) and also by using different concentrations of NADPH (0.01 mM, 0.015 mM, 0.02 mM, 0.04 mM and 0.1 mM) while keeping GSSG concentration constant (1 mM). Enzyme activity was measured for each concentration in triplicates and the specific activity (U/mg protein) was calculated. Michaelis–Menten graphs for variable GSSG (Figure 4.9.A) and variable NADPH (4.10.A) were plotted. Using the same data, Lineweaver-Burk plots were obtained for each variable substrate (Figure 4.9.B and Figure 4.10.B). When GSSG was used as a variable substrate, kinetic parameters were found to be V_m , 220 ± 5 U/mg protein and K_m was found to be 100 ± 7 μ M. Kinetic parameters were found to be 209 ± 8 U/mg protein for V_m and 16 ± 2 μ M for K_m when the variable substrate was NADPH. When the variable substrate was GSSG, substrate inhibition was observed both from Michaelis-Menten and Lineweaver-Burk graphs (Figure 4.9. A. and B).

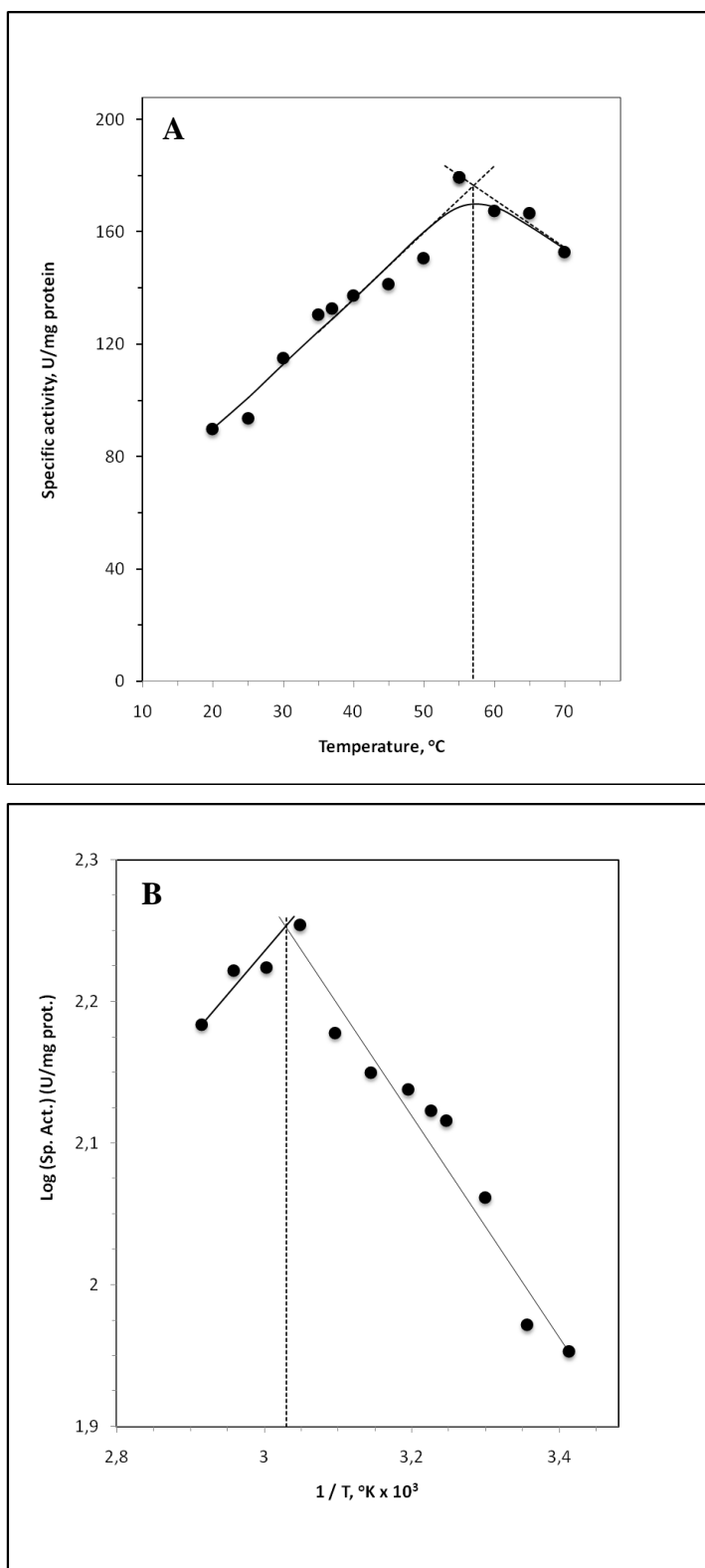


Figure 4.8.A. Specific activity vs. temperature plot. B. Log (Sp.Act.) U/mg protein vs. $1/T$ plot.

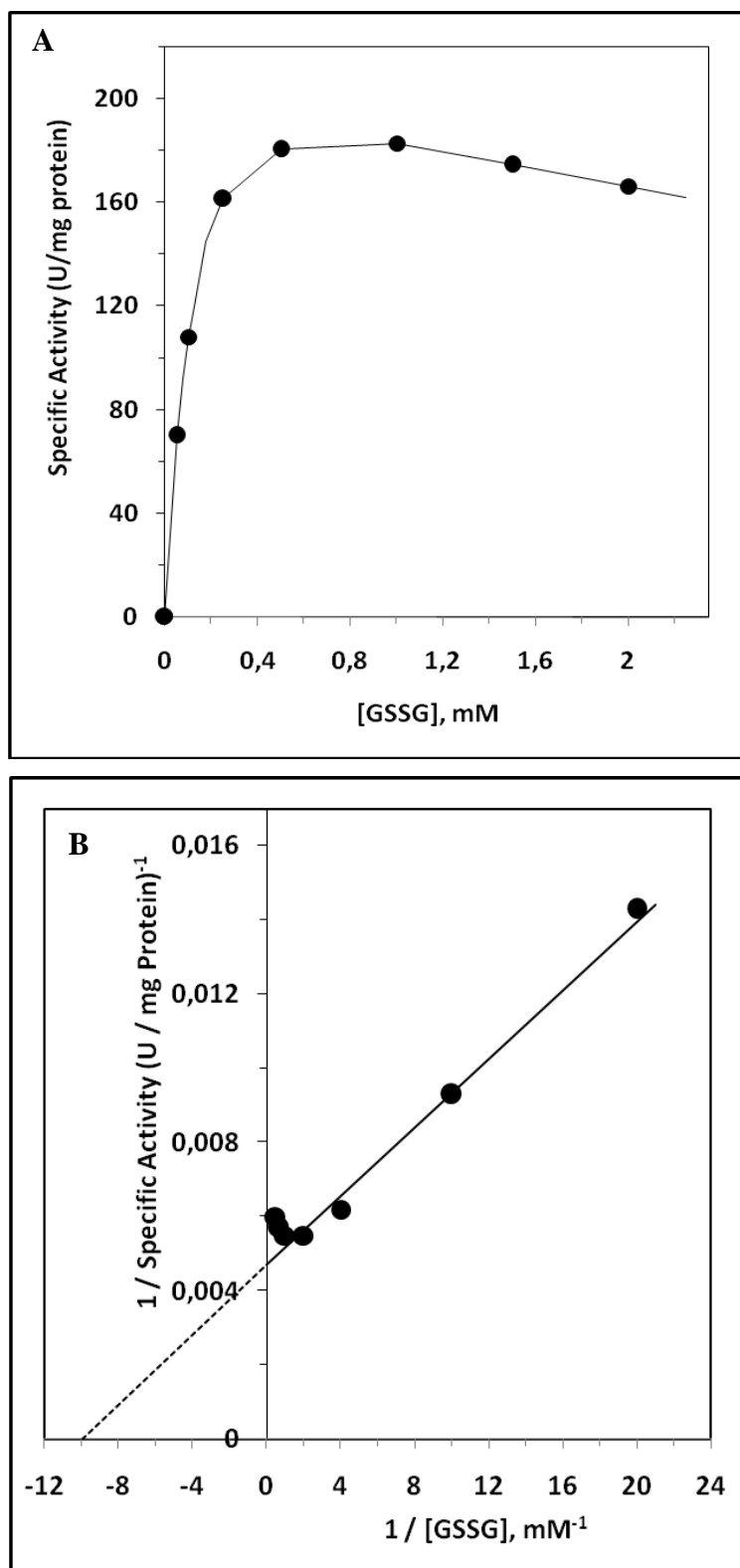


Figure 4.9. Kinetic behavior of glutathione reductase with variable GSSG concentrations (0.05 mM, 0.1 mM, 0.25 mM, 0.5 mM, 1 mM, 1.5 mM and 2 mM). A. Michaelis-Menten plot. B. Lineweaver-Burk plot.

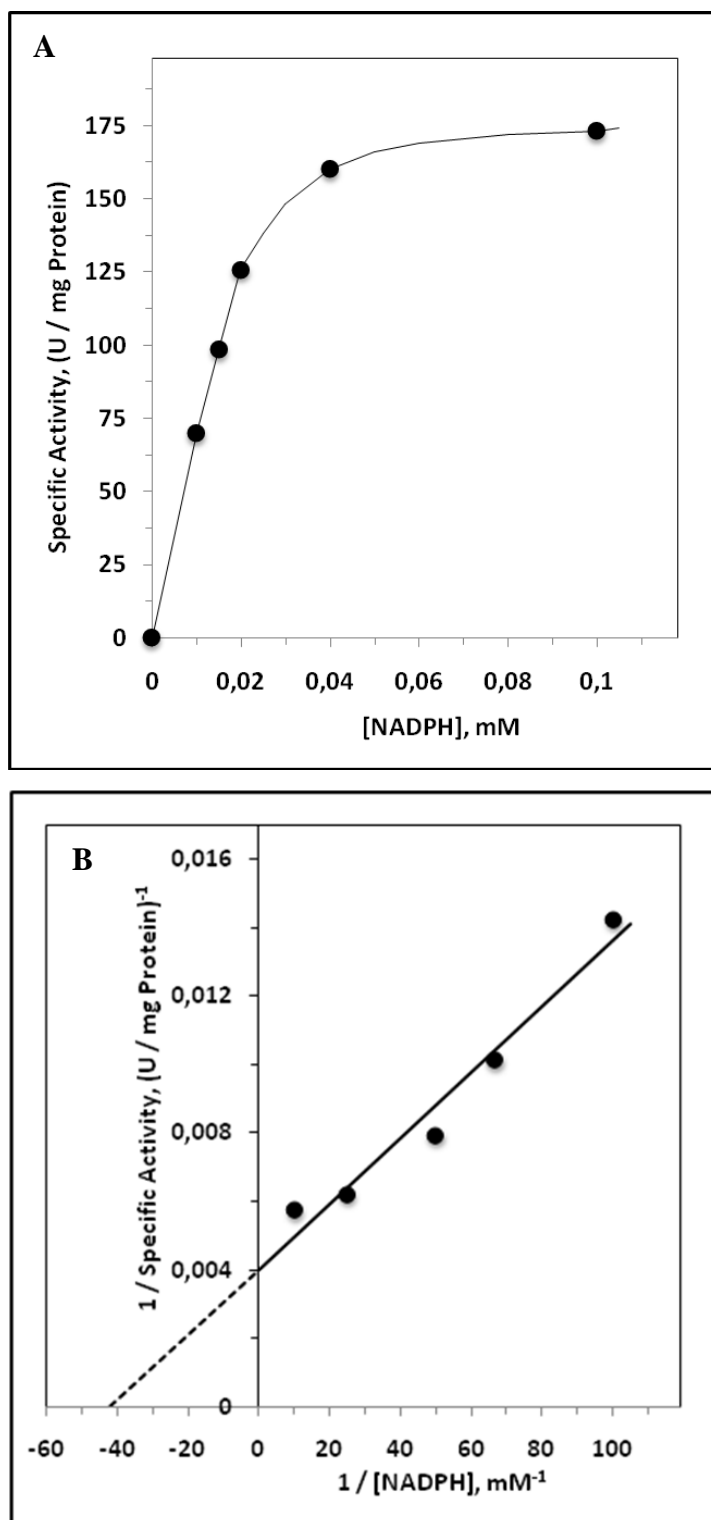


Figure 4.10. Kinetic behavior of glutathione reductase with variable NADPH concentrations (0.01 mM, 0.015 mM, 0.02 mM, 0.04 mM and 0.1 mM). A. Michaelis-Menten plot. B. Lineweaver-Burk plot.

4.4. Inhibitory Kinetic Behaviour of Glutathione Reductase with Fluoxetine

Glutathione reductase activity was measured by using 1 mM GSSG, 0.1 mM NADPH and different concentrations of fluoxetine (0-0.5 mM). Figure 4.11 shows that fluoxetine inhibited glutathione reductase enzyme in a dose dependent manner. There was a continuous decrease in enzyme activity but inhibition did not extend to zero in the concentration range studied. Graph of specific activity versus fluoxetine concentration was plotted and IC_{50} was calculated as 0.73 mM. Four fluoxetine concentrations (0.05 mM, 0.1 mM, 0.2 mM, 0.4 mM) were chosen to be used in the inhibitory kinetic experiments.

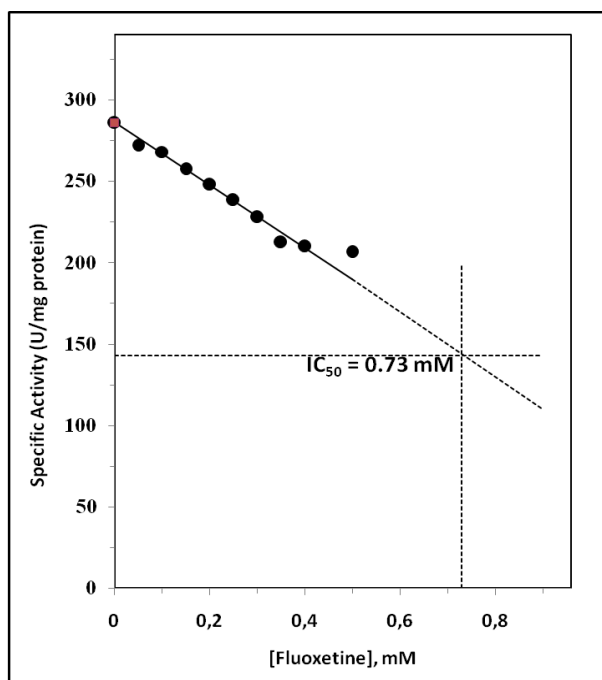


Figure 4.11. Dose dependent inhibition of glutathione reductase by fluoxetine. [GSSG] = 1 mM, [NADPH] = 0.1 mM, [Fluoxetine] = 0 mM, 0.05 mM, 0.1 mM, 0.15 mM, 0.2 mM, 0.25 mM, 0.3 mM, 0.35 mM, 0.4 mM and 0.5 mM.

In the presence of different fluoxetine concentrations (0.05 mM, 0.1 mM, 0.2 mM and 0.4 mM), first NADPH concentration was kept constant (0.1 mM) and variable GSSG concentrations (0.0625 mM, 0.125 mM, 0.25 mM, 0.5 mM and 1 mM) were tested. Then, at fixed 1 mM GSSG concentration, variable NADPH

concentrations (0.01 mM, 0.015 mM, 0.02 mM, 0.04 mM and 0.1 mM) were tested by using the same fluoxetine concentrations. Michaelis Menten, Lineweaver–Burk, Dixon and other graphs were plotted for variable [GSSG] and [NADPH].

When the variable substrate was GSSG, linear mixed-type competitive inhibition was observed with fluoxetine. V_m , K_s , K_i and α values were calculated as 230 ± 3 U/mg protein, 111 ± 5 μ M, 279 ± 32 μ M and 5.48 ± 1.29 , respectively (Figure 4.12 and 4.13).

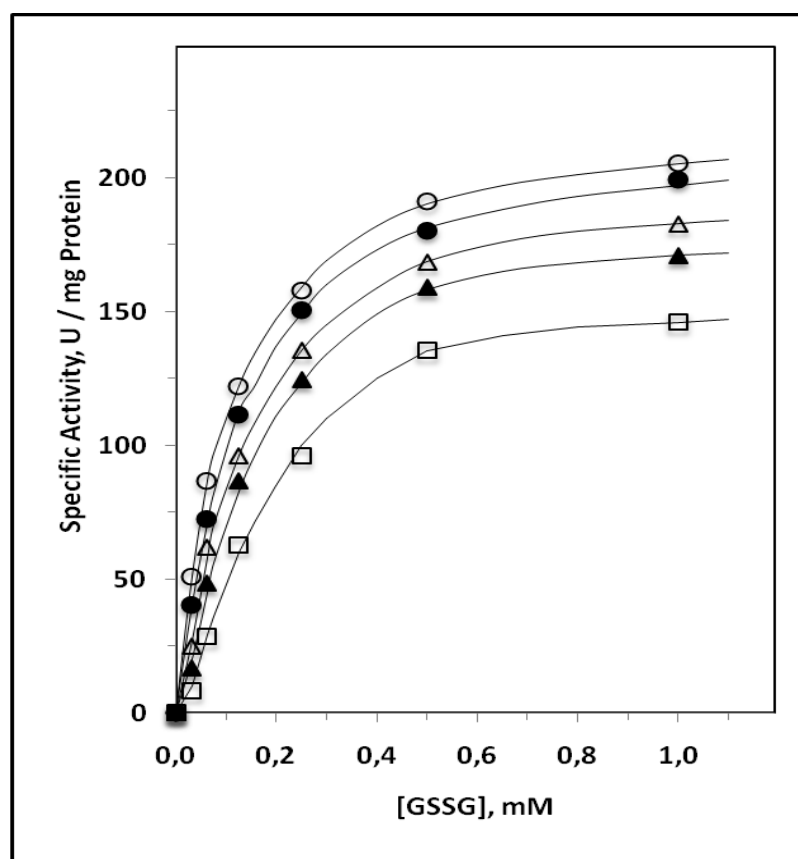


Figure 4.12. Michaelis-Menten plot for glutathione reductase enzyme at different concentrations of fluoxetine by using GSSG as a variable substrate (0.0625 mM, 0.125 mM, 0.25 mM, 0.5 mM and 1 mM). Fluoxetine concentrations were (○) without fluoxetine, (●) 0.05 mM, (△) 0.1 mM, (▲) 0.2 mM and (□) 0.4 mM.

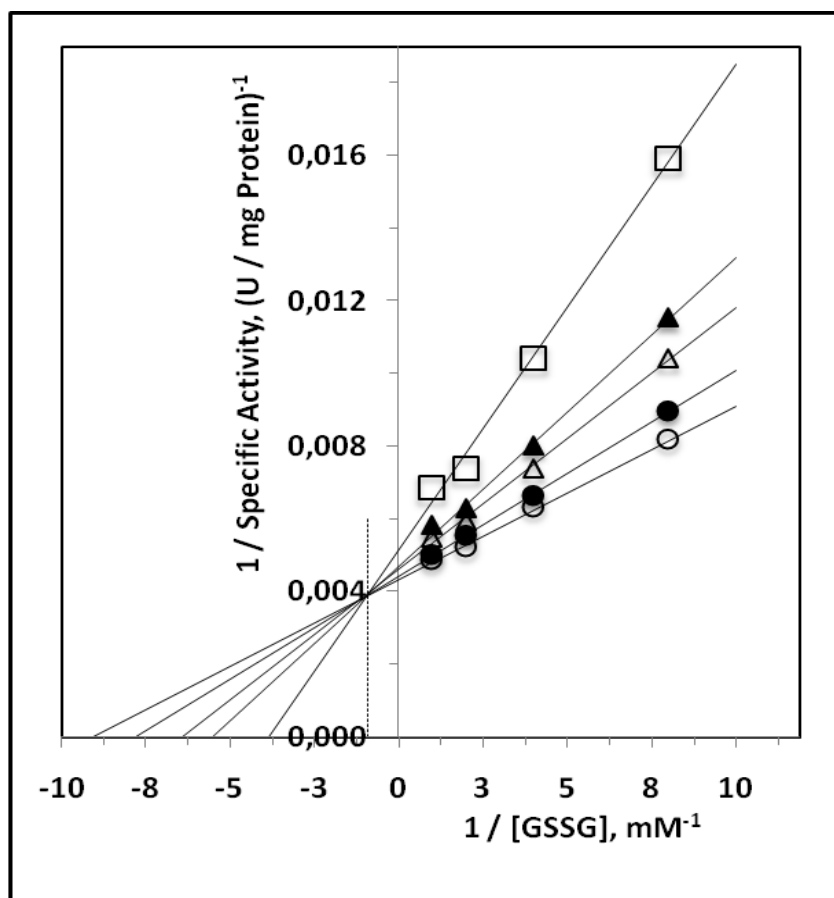


Figure 4.13. Lineweaver-Burk plot for glutathione reductase enzyme at different concentrations of fluoxetine by using GSSG as variable a substrate (0.0625 mM, 0.125 mM, 0.25 mM, 0.5 mM and 1 mM). Fluoxetine concentrations were (○) without fluoxetine, (●) 0.05 mM, (Δ) 0.1 mM, (▲) 0.2 mM and (□) 0.4 mM.

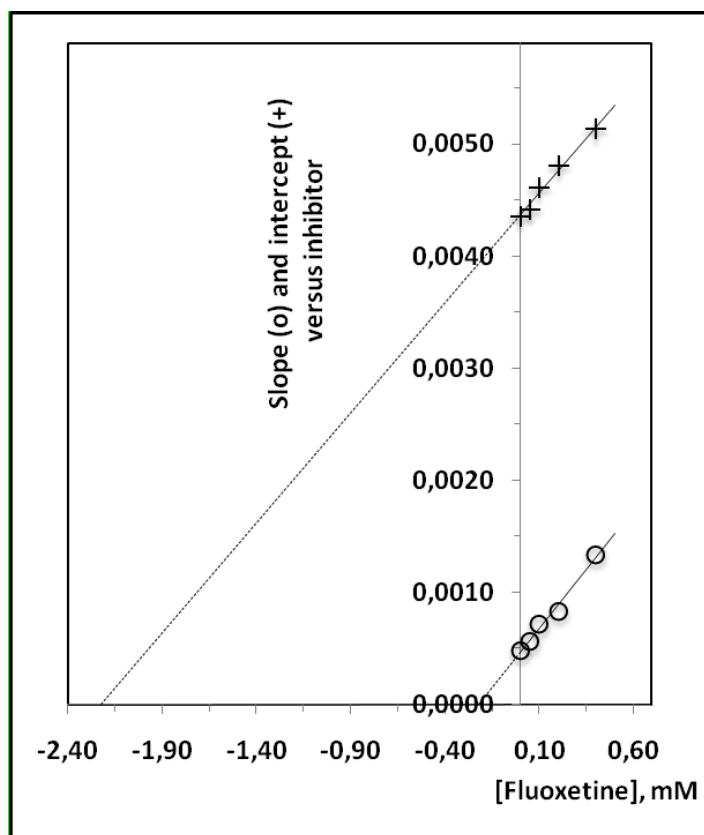


Figure 4.14. Replot of slope and intercept points versus fluoxetine obtained from Figure 4.13.

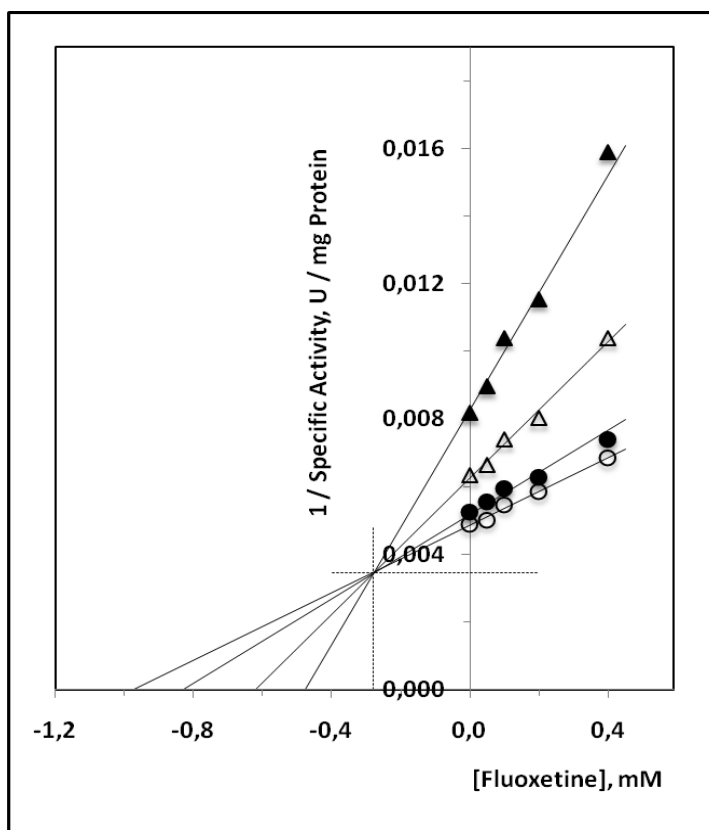


Figure 4.15. Dixon plot for glutathione reductase enzyme at different concentrations of fluoxetine (0, 0.05 mM, 0.1 mM, 0.2 mM and 0.4 mM) by using GSSG as a variable substrate. GSSG concentrations were (\blacktriangle) 0.125 mM, (\triangle) 0.25 mM, (\bullet) 0.5 mM and (\circ) 1 mM.

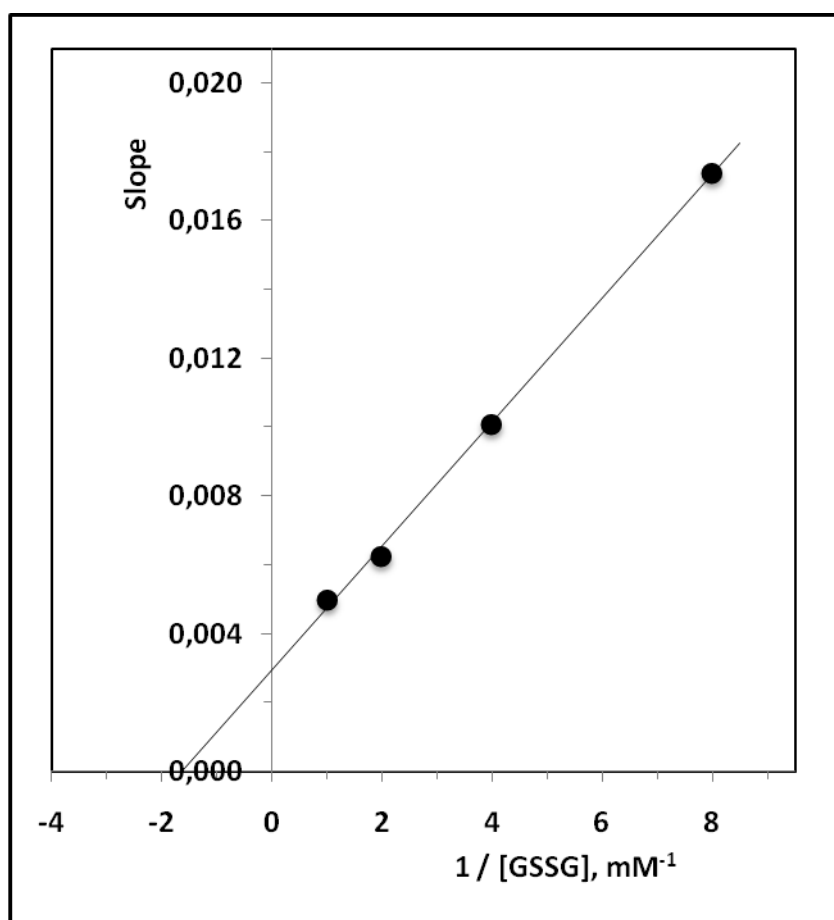


Figure 4.16. Replot of slopes obtained from Figure 4.15 versus $1/[\text{GSSG}]$

When the variable substrate was NADPH, non-competitive inhibition (Figure 4.17 and 4.18) was observed with fluoxetine. V_m , K_m and K_i were calculated as 212 ± 5 U/mg protein, 13.4 ± 0.8 μ M and 879 ± 82 μ M, respectively.

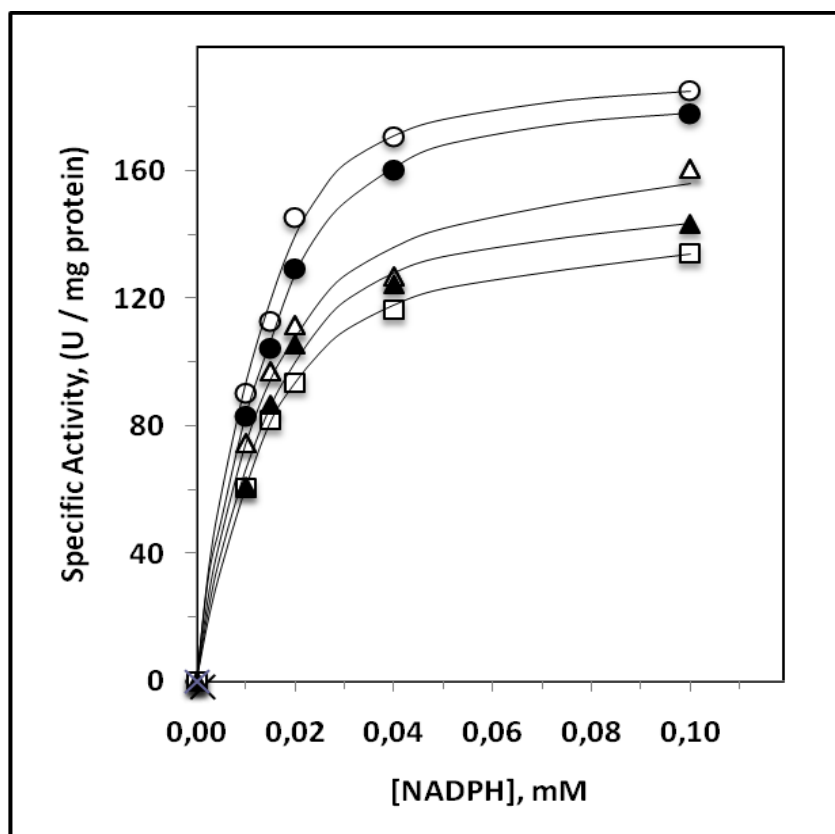


Figure 4.17. Michaelis-Menten plot for glutathione reductase enzyme at different concentrations of fluoxetine by using NADPH as a variable a substrate (0.01 mM, 0.015 mM, 0.02 mM, 0.04 mM and 0.1 mM). Fluoxetine concentrations were (\circ) without fluoxetine, (\bullet) 0.05 mM, (Δ) 0.1 mM, (\blacktriangle) 0.2 mM and (\square) 0.4 mM.

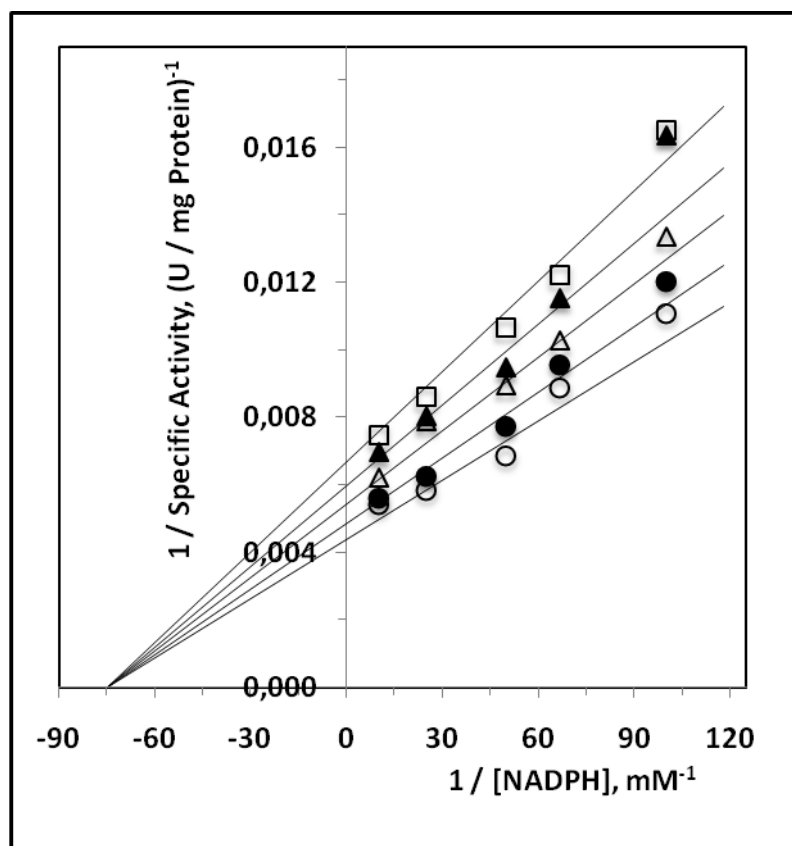


Figure 4.18. Lineweaver-Burk plot for glutathione reductase enzyme at different concentrations of fluoxetine by using NADPH as a variable substrate (0.01 mM, 0.015 mM, 0.02 mM, 0.04 mM and 0.1 mM). Fluoxetine concentrations were (○) without fluoxetine, (●) 0.05 mM, (△) 0.1 mM, (▲) 0.2 mM and (□) 0.4 mM.

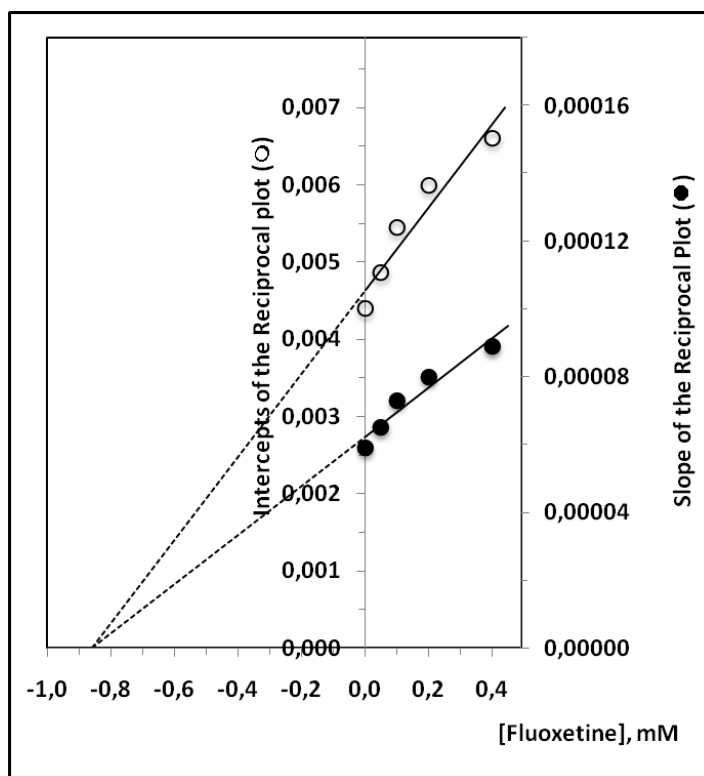


Figure 4.19. Replot of slope and intercept points obtained from Figure 4.18 versus [fluoxetine].

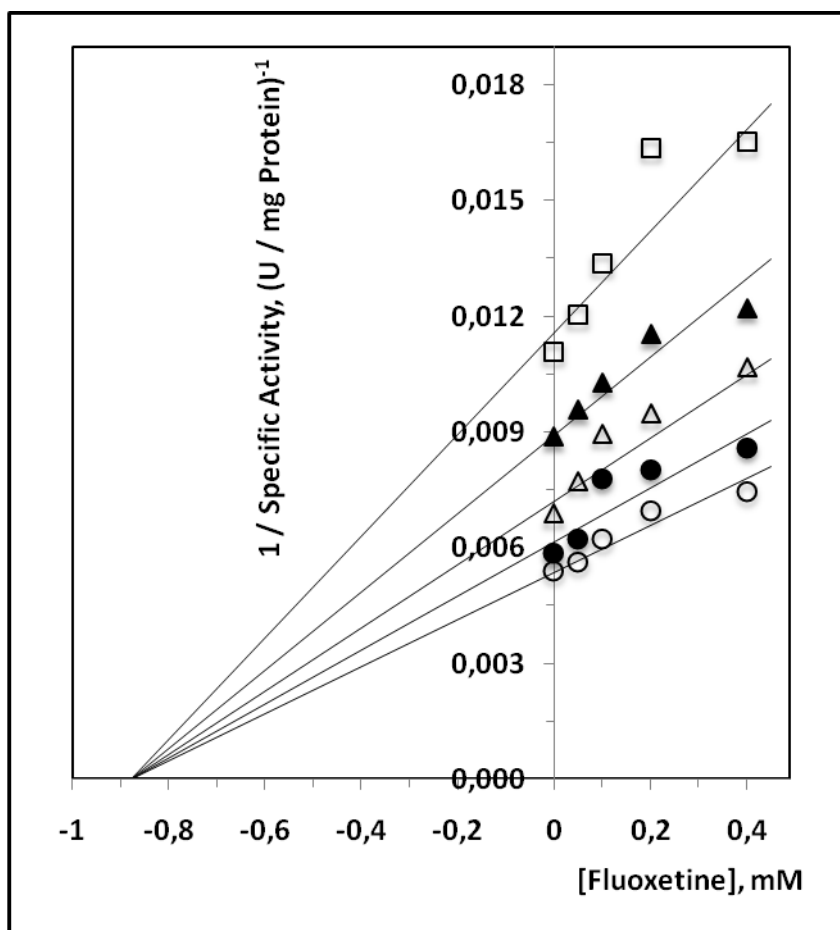


Figure 4.20. Dixon plot for glutathione reductase enzyme at different concentrations of fluoxetine (0, 0.05 mM, 0.1 mM, 0.2 mM and 0.4 mM) by using NADPH as a variable substrate. NADPH concentrations were (□) 0.01 mM, (▲) 0.015 mM, (△) 0.02 mM, (●) 0.04 mM and (○) 0.1 mM.

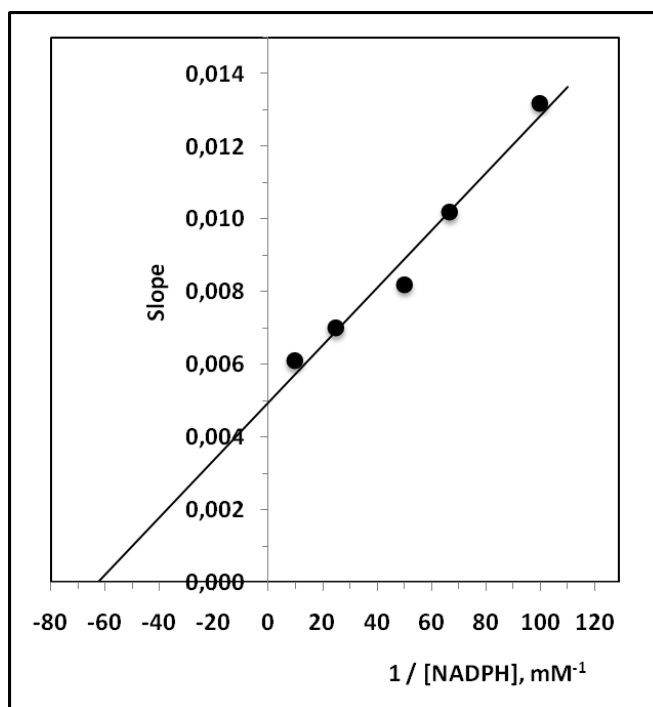


Figure 4.21. Replot of slopes obtained from Figure 4.20 versus $1/[\text{NADPH}]$

5. DISCUSSION

Baker's yeast glutathione reductase (GR) exhibits homology with GR from human serum. They share a common catalytic mechanism with a sole purpose of cellular defense against oxidative stress. These enzymes are composed of three domains; the NADPH binding domain, FAD domain and dimerization domain (Berkholz et al., 2008). In their localization, GR is distinctly investigated to reside in the mitochondria and cytosol where ROS are generated during aerobic metabolism, meaning that highest concentrations of this enzyme is found in these two organelles (Outten and Culotta, 2004). Baker's yeast and human erythrocyte GR has a M_r of 49 kDa and 52 kDa, respectively. Both enzymes are homodimers that catalyze the reduction of GSSG to GSH using FAD as a prosthetic group and NADPH as a reductant (Tandogan et al., 2011; Berkholz et al., 2008). GR is an important ROS cleaning agent and important for redox stability in both human and yeast cells. Its inhibition causes a decline in GSH/GSSG ratio resulting in ROS accumulation and in a long run leads to oxidative stress in the cells which results in several diseases (Barker et al., 1996; Tandogan et al., 2011). Human GR is known to have 461 amino acid residues whereas yeast GR is known to exhibit 467 amino acids. Both GRs contain FAD as prosthetic group and although comparison of GR in yeast and human reveals 49.8% identity, human GR contains an inter subunit disulphide bond (Karplus and Schulz 1987; Collinson and Dawes 1995).

During our research, baker's yeast GR was procured commercially. Two types of gel electrophoresis (native and SDS-PAGE) were carried out in order to determine enzyme purity and subunit molecular weight. Different staining techniques (Coomassie Brilliant Blue R-250, silver and activity stainings) were conducted on gels in order to visualize protein bands. A single protein band in native gel (Figures 4.2 and 4.3) confirmed the purity of the enzyme. Similar results were also obtained by Mavis and Stellwagen in purification of baker's yeast GR (Mavis and Stellwagen, 1968). Two monomeric subunits which are undoubtedly identical gave also a single protein band in SDS-PAGE (Figures 4.4. and 4.5.A). Molecular weight of each subunit was calculated as 49 kDa. Similar results were obtained by Hou et al. in the detection of GR after electrophoresis on native and SDS gels (Hou et al., 2004). Single protein bands in both native and SDS-PAGE were consistent with the studies

of Ogus and Ozer's on purification of NADP-free glutathione disulphide reductase from human erythrocytes (Ogus and Ozer, 1998).

Characterization of GR enzyme was accomplished by determining the optimum pH and temperature. In order to obtain the optimum pH, zero buffer extrapolation method was used (Landqvist, 1955). The GR enzyme activity at zero [buffer] was found by extrapolation. Using the activities at zero buffer concentration (Figure 4.6), activity versus pH graph was plotted and from the graph a value for pH optimum was plotted and from the graph a value for pH optimum was found to be 7.65 (Figure 4.7). Optimum temperature, energy of activation and Q_{10} were calculated as 57°C, 3,544 calories and 1.26, respectively. The pH and temperature optimum values were in accordance with the results obtained by Erat et al. for the glutathione reductase purified from bovine erythrocytes. The bovine enzyme's optimum pH and temperature were found to be 7.3 and 55°C, respectively (Erat et al., 2003). Can et al, reported a pH optimum of 6.5 and a temperature optimum of 65°C for rat kidney glutathione reductase (Can, B et al., 2010). The inconsistency in the optimum pH and temperature values of baker's yeast and rat kidney GR enzymes might be explained by the differences in the functions of those tissues.

To determine the substrate kinetic parameters, different concentrations of NADPH and GSSG were tested. The GR activities at fixed [NADPH] (0.1 mM), variable [GSSG] (0.05 mM, 0.1 mM, 0.25 mM, 0.5 mM, 1 mM, 1.5 mM and 2 mM) and at fixed [GSSG] (1 mM) variable NADPH (0.01 mM; 0.015 mM; 0.02 mM; 0.04 mM and 0.1 mM) were measured. The V_m and K_m values for GSSG and NADPH were found to be 220 ± 5 U/mg protein and 100 ± 7 μ M (Figure 4.9) and 209 ± 8 U/mg protein and 16 ± 2 μ M (Figure 4.10), respectively.

In the preceding study, our main interest was primarily on the GR inhibition by fluoxetine which may be very useful during the treatment of mental disordered and depressed individuals. Increased fluoxetine treatment in the long run may deplete the activity of the GR resulting in oxidative stress, the leading factor of many diseases. Consequently, we analyzed the kinetic action of GR in the presence of fluoxetine.

Activity measurements were carried out by using different fluoxetine concentrations (0-0.5 mM), at constant GSSG (1 mM) and NADPH (0.1 mM)

concentrations. However, fluoxetine inhibited glutathione reductase enzyme in a dose-dependent manner and half inhibition, IC_{50} , was calculated as 0.73 mM (Figure 4.11), inhibition did not reach to zero in the concentration range studied. For further studies, four fluoxetine concentrations (0.05 mM, 0.1 mM, 0.2 mM and 0.4 mM) were selected, due to the fact that the inhibition pattern within this range was linear. Enzyme activity was further measured using the same fluoxetine concentrations but with variable GSSG and fixed NADPH (0.1 mM) as well as variable NADPH and fixed GSSG (1 mM). GSSG concentrations ranged between 0.0625-1 mM when [NADPH] was constant (0.1 mM) and NADPH concentrations ranged between 0.01-0.1 mM, when [GSSG] was constant (1 mM). At fixed NADPH (0.1 mM) and at variable GSSG, fluoxetine inhibited glutathione reductase enzyme in a linear competitive mixed type manner. Substrate dissociation constant (K_s), inhibition constant (K_i) and alpha (α) values were calculated as $111 \pm 5 \mu\text{M}$, $279 \pm 32 \mu\text{M}$ and 5.48 ± 1.29 , respectively (from intersection points and statistical analysis (Statistica)) (Figure 4.12 and 4.13). At fixed [GSSG] (1 mM) and at variable [NADPH], fluoxetine inhibited GR non-competitively. Michaelis constant (K_m) and inhibition constant (K_i) were calculated as $13.4 \pm 0.8 \mu\text{M}$ and $879 \pm 82 \mu\text{M}$, respectively (Figure 4.17 and 4.18). According to the inhibition type at variable GSSG, it was discovered that fluoxetine did not bind to the GSSG or NADPH binding sites but rather it showed competitive action with GSSG for its binding site due to the fact fluoxetine bound much closer to the GSSG binding site. However, as regards to the inhibition type at variable NADPH, fluoxetine exhibited non-competitive inhibition, this could be explained by the conformational change of the glutathione reductase enzyme due to the binding of fluoxetine.

The selective serotonin reuptake inhibitor, fluoxetine, is a widely prescribed medication for depression (Kashanian et al., 2012). Fluoxetine was disclosed to inhibit GR activity in erythrocytes meaning that in spite of the various valuable action of fluoxetine, it may also affect the transportation of oxygen and hemoglobin function throughout the cells (Adzic et al., 2011).

Increased GSH levels are known to correlate with proliferation and cell cycle progression. Therefore inhibition of GR enzyme can be beneficial especially in cancer patients during chemotherapy, due to the fact that a decrease in GR renders

the cell susceptible to free radical attacks which is beneficial in the destruction of cancer cells. It also has deleterious effects in normal individuals and others affected with certain diseases (Traverso et al., 2013). For instance, GR is an essential flavoenzyme, present in different cells of the living system like RBCs, heart cells, brain cells with a primary role of protecting cells from oxidative injury. Impairment of this enzyme will expose these cells to oxidative damage which can lead to different health complications like anemia, cardiovascular diseases, neurodegenerative diseases (Rodríguez et al., 2005).

In RBCs, GR protects the protein molecule (hemoglobin) which is very crucial for oxygen transportation. Inhibition of GR will result in anemia due to free radical attack on the membrane (Chang et al., 1978). However, ROS accumulation has been reported in neurodegenerative cases like Parkinson's disease and reduced glutathione is known to be essential for safeguarding the brain from free radical attacks. Since GR is very important for GSH/GSSG homeostasis, inhibition of this enzyme will also result in ROS accumulation in Parkinson's disease patients (Aoyama and Nakaki, 2013; Dias et al., 2013).

In vivo studies reported a decline in the levels of certain antioxidant enzymes including GR after treatment with antidepressant fluoxetine. According to Singh et al., treatment of mice with fluoxetine revealed a remarkable impact on GR and SOD levels only in the first two days of fluoxetine treatment. Followed by chronic swim test, rodents exhibited a significant decrease in the brain levels of antioxidant enzymes including GR and SOD and also an increase in lipid peroxidation as a result of oxidative stress (Singh et al., 2002). However, Herbet et al. reported an increase in the blood level of GR activity after 14 day of combined treatment of fluoxetine (10 mg/kg) and rosuvastatin (10 mg/kg) *in vivo*. Another 14 days of treatment with only fluoxetine exhibited no effect at all on the GR, GPx and the total antioxidant status (TAS) in rat's blood. The increase in the activity of GR, GPx and ROS generation, could be explained by a long term combined treatment with fluoxetine and rosuvastatin in rats (Herbet et al., 2015).

Downregulation of GR has been reported in Asian clam *Corbicular fluminea* after exposure to different concentrations of fluoxetine (0.5, 5, and 50 µg/L) for 30 days. Apart from that, the decrease in SOD was also noted with 5 and 50 µg/L doses

and an increase in catalase enzyme was reported in the same concentrations. These findings also demonstrated an induced oxidative stress as result of fluoxetine treatment in *C. fluminea* (Chen et al., 2015).

Apart from the fact that fluoxetine has been reported to inhibit GR enzyme. The interaction of fluoxetine with placental glutathione-S-transferase- π has been reported (Dalmizrak et al., 2016) since glutathione S-transferase- π is expressed even at 12 weeks of gestation (Carder et al., 1990). Certain *in vivo* experiments has shown that fluoxetine can cross the placenta and is distributed within the embryo during the organogenesis and post-organogenesis period (Pohland et al., 1989; Hendrick et al., 2003). The fact that this SSRI crosses the placenta, may cause certain effects on the fetus as a result of its interaction with the placental glutathione S-transferase- π enzyme (Morrison et al., 2005; Dalmizrak et al., 2016; Kaihola et al 2016).

Inhibition of GR in different tissues like brain, liver, heart and blood will expose these cells to oxidative attacks most especially the brain which happens to be the important organ with highest oxygen consumption. GR inhibition in the brain has been linked to a progressive increase in neurodegenerative diseases. Similarly, GR inhibition in the heart, liver and blood cells will lead to cardiovascular and hepatic diseases. In case of the inhibition of GR in blood cells, hemolytic anemia might be observed as well (Rodríguez et al., 2005; Waggiallah et al., 2011).

Pacher and Kecskemeti also reported an inhibitory effect of fluoxetine treatment on cardiac and vascular Na^+ , Ca^{2+} and K^+ channels in different mammalian and human cardiovascular preparations. Several studies has also linked arrhythmia and orthostatic hypotension in patients who lacked cardiovascular diseases with the use of these SSRI antidepressants showing that fluoxetine may also exhibit certain cardiac side effects during treatment (Pacher and Kecskemeti, 2004).

Certain studies have reported the beneficial effects of fluoxetine in the treatment of depression and few findings have also shown the adverse and deleterious effects of fluoxetine treatment in cells as a result of free radical invasion resulting in pro-oxidant and antioxidant imbalance which can cause an increase in the intensity of certain health complications. It is also important to know that fluoxetine also enhances behavioral activity by suppressing the generation of soluble β -amyloid (Wang et al., 2004).

Fluoxetine is a confirmed antidepressant drug and its inhibitory effect on GR can also be useful during chemotherapy treatment since high GSH level as a result of increased GR level makes cancer cells more resistant to chemotherapy (Ballatori et al., 2009). Other antidepressant drug, amitriptyline has also been reported to play a minor supporting role on the potency of anticancer drugs due to their role in the inhibition of glutathione-S-transferases- π (GST- π) and glutathione S-transferases alpha (GST- α) (Kulaksiz-Erkmen et al., 2013), since the enzyme glutathione-S-transferase has been linked to anticancer drug resistance (Townsend and Tew, 2003) and most importantly its isozyme (GST- π) which is over expressed in cancer cells is known to be related with chemotherapy resistance in breast cancer (Su et al., 2003).

6. CONCLUSION

In this study, inhibitory effect of fluoxetine on baker's yeast glutathione reductase (GR) was analyzed. Native and SDS-PAGE were performed in order to ascertain enzyme purity. Characterization of GR was further carried out to determine the optimum pH and temperature of the enzyme. Kinetic experiments were also conducted by using different concentrations of GSSG and NADPH to calculate the V_m and K_m of the enzyme. Eventually, the inhibitory effect of fluoxetine was tested by using different concentrations of fluoxetine.

Coomassie Brilliant Blue R-250, silver and activity stainings of the native gel produced a single protein band. SDS-PAGE was used to determine the molecular weight of the enzyme; single protein band with a molecular weight of 49 kDa was obtained on SDS-PAGE.

Optimum pH and temperature of the enzyme was found to be 7.65 and 57°C, respectively. Energy of activation and temperature coefficient (Q_{10}) were 3,544 calories and 1.26.

Fluoxetine inhibition of GR was dose-dependent with IC_{50} calculated as 0.73 mM. When GSSG was used as a variable substrate, fluoxetine inhibited glutathione reductase enzyme in a linear competitive mixed type manner with K_s , K_i and α values of $111 \pm 5 \mu\text{M}$, $279 \pm 32 \mu\text{M}$ and 5.48 ± 1.29 , respectively. When NADPH was the variable substrate, inhibition was non-competitive. A value of $13.4 \pm 0.8 \mu\text{M}$ for K_m and a value of $879 \pm 82 \mu\text{M}$ for K_i were obtained.

Further investigations on the mechanism of action of fluoxetine on GR and its clinical use should be carried out since GR enzyme depletion is accountable to the build-up of ROS and later oxidative stress which happens to be the pathologic hallmark of certain diseases.

REFERENCES

- Abdul-Razzak, K.K., Almomany, E.M., Nusier, M.K., Obediat, A.D., Salim, A.M. (2008). Antioxidant vitamins and glucose-6-phosphate dehydrogenase deficiency in full-term neonates. *Ger Med Sci.* 24 (6): 1-5.
- Adzic, M., Djordjevic, J., Mitic, M., Simic, I., Rackov, G., Djordjevic, A. et al. (2011). Fluoxetine decreases glutathione reductase in erythrocytes of chronically isolated wistar rats. *Acta Chin Slov.* 58 (4): 785-91.
- Aminian, M., Nabatchian, F., Vaisi-Raygani, A., Torabi, M. (2013). Mechanism of Coomassie Brilliant Blue G-250 binding to cetyltrimethylammonium bromide: an interference with the Bradford assay. *Anal Biochem.* 434 (2): 289-91.
- Anderson, F., Schade, R., Suissa, S., Garbe, E. (2009). Long-term use of antidepressant for depressive disorders and the risk of diabetes mellitus. *Am J Psychiatry.* 166 (5): 591-8.
- Aoyama, K. and Nakaki, T. (2013). Impaired glutathione synthesis in neurodegeneration. *Int J Mol Sci.* 14 (10): 21021-44.
- Arora, K., Ahmad, R., Srivastava, A.K. (2013). Purification and characterization of glutathione reductase (E.C.1.8.1.7) from bovine filarial worms' setaria cervi. *J Parasite Dis.* 37 (1): 94-104.
- Ballatori, N., Krance S.M., Notenboom, S., Shi S., Tieu, K., Hammond, C.L. (2009). Glutathione dysregulation and the etiology and progression of human diseases. *Biol Chem.* 390 (3): 191-214.
- Barker, J.E., Heales, S.J., Cassidy, A., Bolanos, J.P., Land J.M., Clark, J.B. (1996). Depletion of brain glutathione results in a decrease of glutathione reductase activity; an enzyme susceptible to oxidative damage. *Brain Res.* 716 (1-2): 118-22.
- Beal, M.F. (1995). Aging, energy and oxidative stress in neurodegenerative diseases. *Anal Neurol.* 38 (3): 357-66.

- Berkholz, D.S., Faber, H.R., Savvides, S.N., Karplus, P.A. (2008). Catalytic cycle of human glutathione reductase near 1Å resolution. *J Mol Biol.* 382 (2): 371-84.
- Beutler, E. (1969). Effect of flavin compounds on glutathione reductase activity: in vivo and in vitro studies. *J Clin Invest.* 48 (10): 1957-66.
- Birben, E., Sahiner, U.M., Sackesen, C., Erzurum, S., Kalayci, O. (2012). Oxidative stress and antioxidant defense. *World Allergy Organ. J.* 5(1): 9-19.
- Birmaher, B., Axelson, D.A., Monk, K., Kalas, C., Clark, D.B., Ehmann, M., et al. (2003). Fluoxetine for the treatment of childhood anxiety disorders. *J Am Acad Child Adolesc Psychiatry.* 42 (4): 415-23.
- Blum, H., Beier, H., Gross, H.J. (1987). Improved silver staining of plant proteins, RNA and DNA in polyacrylamide gels. *Electrophoresis.* 8 (2): 93-99.
- Bradford, M.M. (1976). A rapid sensitive method for the quantification of microgram quantities of protein utilizing the principle of protein-dye binding. *Analytical Biochemistry.* 72: 248-254.
- Can, B., Kulaksiz Erkmen, G., Dalmizrak, O., Ogus, I.H., Ozer, N. (2010). Purification and characterization of rat kidney glutathione reductase. *Protein J.* 29 (4): 250-6.
- Carder, P.J., Hume, R., Fryer, A.A., Strange, R.C., Lauder, J., Bell, J.E. (1990). Glutathione-S-transferase in human brain. *Neuropathol Appl Neurobiol.* 16 (4): 293-303.
- Carlberg, I., Mannervik, B. (1988). Purification of flavoenzyme glutathione reductase from rat liver. *J Biol Chem.* 250 (14): 5475-80.
- Chang, J.C., Vander Hoeven, L.H., Haddox, C.H. (1978). Glutathione reductase in red blood cells. *Ann Clin Lab Sci.* (1): 23-9.
- Chen, H., Zha, J., Yuan, L., Wang, Z. (2015). Effects of fluoxetine on behaviour, antioxidant enzyme systems, and multixenobiotic resistance in the Asian clam *Corbicula fluminea*. *Chemosphere.* 119: 856-62.

Chen, X., Guo, C., Kong, J. (2012). Oxidative stress in neurodegenerative diseases. *Neural Regen Res.* 7 (5): 376-85.

Coccaro, E.F., Kavoussi, R.J. (1997). Fluoxetine and impulsive aggressive behaviour in personality disordered subjects. *Arch Gen Psychiatry.* 54 (12): 1081-8.

Collinson, L.P, Dawes, I.W. (1995). Isolation, characterization and overexpression of of the yeast gene, GLR1, encoding glutathione reductase. *Gene.* 156(1): 123-7.

Copley, S.D., Dhillon, J.K. (2002). Lateral gene transfer and parallel evolution in the history of glutathione biosynthesis genes. *Genome Biol.* 3 (5): 1-16.

Curello, S., Ceconi, C., Bigoli, C., Ferrari, R., Albertini, A., Guarnieri, C. (1985). Changes in the cardiac glutathione status after ischemia and reperfusion. *Experientia.* 41 (1): 42-3.

Dalmizrak, O., Kulaksiz-Erkmen, G., Ozer, N. (2016). Fluoxetine-induced toxicity results in human placental glutathione S-transferase- π (GST- π) dysfunction. *Drug Chem Toxicol.* 39 (4): 439-44.

Daniel, W.A., Wójcikowski, J. (1997). Interaction between promazine and antidepressants at the level of cellular distribution. *Pharmacol Toxicol.* 81 (6): 259-64.

Day, B.J. (2009). Catalase and glutathione peroxidase mimics. *Biochem Pharmacol.* 77(3): 283-96.

Deponte, M. (2013). Glutathione catalysis and the reaction mechanisms of glutathione-dependent enzymes. *Biochim Biophys Acta.* 1830 (5): 3217-66.

Dhalla, N.S., Temsah, R.M, Netticadan, T. (2000). Role of oxidative stress in cardiovascular diseases. *J Hypertens.* 18 (6): 655-73.

Dias, V., Juun, E., Mouradian, M.M. (2013). The role of oxidative stress in Parkinson's disease. *J Parkinsons Dis.* 3 (4): 461-91.

Djordjević, V.B., Zvezdanović, L., Cosić, V. (2008). Oxidative stress in human disease. *Srp Arh Celok Lek.* 136 (2): 158-65.

- Enwonwu, C.O. (1988). Nutritional support in sickle cell anemia: theoretical considerations. *J Natl Med Assoc.* 80 (2): 139-44.
- Erat M, Sakiroglu H, Ciftci M. (2003). Purification and characterization of glutathione reductase from bovine erythrocytes. *Prep Biochem Biotechnol.* 33 (4): 283-300.
- Espinosa-Diez, C., Miguel, V., Mennerich, D., Kietzmann, T., Sánchez-Pérez, P., Cadenas, S., et al. (2015). Antioxidant responses and cellular adjustments to oxidative stress. *Redox Biol.* 6: 183-97.
- Farnam, A., Goreishizadeh, M.A., Farhang, S. (2008). Effectiveness of fluoxetine on various subtypes of obsessive-compulsive disorder. *Arch Ira Med.* 11 (5): 522-5.
- Ferguson, J.M. (2001). SSRI antidepressant medications: Adverse effects and tolerability. *Prim Care Companion J Clin Psychiatry.* 3 (1): 22-27.
- Fjordside, L., Jeppesen, U., Eap, C.B., Powell, K., Baumann, P., Brøsen, K. (1999). The stereo selective metabolism of fluoxetine in poor and extensive metabolizers of sparteine. *Pharmacogenetics.* 9 (1): 56-60.
- Galli, F., Battistoni, A., Gambari, R., Pompella, A., Bragonzi, A., Pilolli, F., et al. (2012). Oxidative stress and antioxidant therapy in cystic fibrosis. *Biochim Biophys Acta.* 1822 (5): 690-713.
- Giacco, F., Brownlee, M. (2010). Oxidative stress and diabetic complications. *Circ Res.* 107 (9): 1058-70.
- Graubaum, W.B. (1981). *Handbook for Forensic Individualization of Human Blood and Blood Stains.* Berkeley, CA: Sartorius GmbH.
- Griese, M., Kappler, M., Eismann, C., Ballmann, M., Junge, S., Rietschel, E. (2013). Inhalation treatment with glutathione in patients with cystic fibrosis. A randomized clinical trial. *Am J Respir Crit Care Med.* 188 (1): 83-9.

Grntzalis, K., Georgiou, C. D., Schneider, Y. J. (2015). An accurate and sensitive Coomassie Brilliant Blue G-250-based assay for protein determination. *Anal Biochem.* 480:28-30.

Kalkan, I.H., Suher, M. (2013). The relationship between the level of glutathione impairment of glucose metabolism and complications of diabetes mellitus. *Pak J Med Sci.* 29 (4): 938-42.

Hames, B.D., ed. (1998). *Gel electrophoresis of proteins: A practical approach.* New York: Oxford University Press.

Harrison, D.G., Gongora, M.C. (2009). Oxidative stress and hypertension. *Med Clin North Am.* 93 (3): 621-35.

Hendrick, V., Stowe, Z. N., Altshuler, L.L., Hwang, S., Lee, E., Haynes, D. (2003) Placental passage of antidepressant medications. *Am J Psychiatry.* 160 (5): 993-6.

Henneberg, R., Otuki, M.F., Furman, A.E., Hermann, P., do Nascimento, A.J., Leonart, M.S. (2013). Protective effects of flavonoids against reactive oxygen species production in sickle cell anemia patients treated with hydroxyurea. *Rev Bras Hematol Hemoter.* 35 (1): 52-5.

Herbet, M., Gawrońska-Grzywacz, M., Jagiello-Wójtowicz, E. (2015). Evaluation of selected biochemical parameters of oxidative stress in rats pretreated with rosuvastatin and fluoxetine. *Acta Pol Pharm.* 72 (2): 261-5.

Hou, W.C., Liang, H.J., Wang, C.C., Liu, D.Z. (2004). Detection of glutathione reductase after electrophoresis on native or sodium dodecyl sulfate polyacrylamide gels. *Electrophoresis.* 25 (17): 2926-31.

Ismail, N.A., Okasha, S.H., Dhawan, A., Abdel-Rahman, A.O, Shaker, O.G, Sadik, N.A. (2010). Antioxidant enzymes activities in hepatic tissue from children with chronic cholestatic liver disease. *Saudi J Gastroenterol.* 16 (2): 90-4.

Isaac, R., Boura-halfon, S., Gurevitch, D., Shainskaya, A., Levkovitz, Y., Zick, Y. (2013). Selective serotonin reuptake inhibitors (SSRIs) inhibit insulin secretion and action in pancreatic β -cells. *J Biol Chem.* 288 (8): 5682-93.

Johnson, R.D., Lewis, R.J., Angier, M.K. (2007). The distribution of fluoxetine in human fluids and tissues. *J Anal Toxicol.* 31 (7): 409-14.

Jordana, S.B., Bruno J.G., Maria Eugênia C.Q. (2011). Enantioselective analysis of fluoxetine and norfluoxetine in plasma samples by protein precipitation and liquid chromatography with fluorescence detection. *J Braz Chem Soc.* 22 (7): 1221-1228.

Kaihola, H., Yaldir, F.G., Hreinsson, J., Hörnaeus, K., Bergguist, J., Olivier, J.D. et al., (2016). Effects of fluoxetine on human embryo development. *Front Cell Neurosci.* 10: 160.

Kakkar, A.K., Dahiya, N. (2015). Management of Parkinson's disease current and future pharmacotherapy. *Eur J Pharmacol.* 5 (750): 74-81.

Kamerbeek, N.M., van Zwieten, R., de Boer, M., Morren, G., Vuil, H., Bannink, N., et al. (2007). Molecular basis of glutathione reductase deficiency in human blood cells. *Blood.* 109 (8): 3560-6.

Kaneko, T., Luchi, Y., Kobayashi, T., Fujii, T., Saito, H., Kurachi, H. et al. (2002). The expression of glutathione reductase in the male reproductive system of rats supports the enzymatic basis of glutathione function in spermatogenesis. *Eur J Biochem.* 269 (5): 1570-8.

Karplus, P. A., Schulz, G.E. (1987). Refined structure of glutathione reductase at 1.54 Å resolution. *J Mol Biol.* 195 (3): 701-29.

Kashanian, S., Javanmardi, S., Chitsazan, A., Omidfar, K., Paknejad, M. (2012). DNA-binding studies of fluoxetine antidepressant. *DNA Cell Biol.* 31(7): 1349-55.

Kawadler, J.M., Kirkham, F.J., Clayden, J.D., Hollocks, M. J., Seymour, E.L., Edey, R., et al. (2015). White matter damage relates to oxygen saturation in children with sickle cell anemia without silent cerebral infarcts. *Stroke.* 46 (7): 1793-9.

Kim, G.H., Kim, J.E., Rhie, S.J., Yoon, S. (2015). The role of oxidative stress in neurodegenerative disease. *Exp Neurobiol.* 24 (4): 325-40.

- Kulaksiz-Erkmen, G., Dalmizrak, O., Dincsoy-Tuna, G., Dogan, A., Ogus, I. H., Ozer, N. (2013). Amitriptylin may have a supporting role in cancer treatment by inhibiting glutathione S-transferase pi (GST- π) and alpha (GST- α). *J Enzyme Inhib Med Chem.* 28 (1): 131-6.
- Kullyev, A., Dempsey, C.M., Miller, S., Kuan, C.J., Hapiak, V.M., Komuniecki, R.W. et al. (2010). A genetic survey of fluoxetine action on synaptic transmission in *Caenorhabditis elegans*. *Genetics.* 186 (3): 929-41.
- Krauth-Siegel, R.L., Blatterspiel, R., Saleh, M., Schiltz, E., Schirmer, R.H. et al. (1982). Glutathione reductase from human erythrocytes. The sequences of the NADPH domain and of the interface domain. *Eur J Biochem.* 121 (2): 259-67.
- Laemmli, U.K. (1970). Cleavage of structural proteins during the assembly of the head of bacteriophage T4. *Nature.* 227 (5259): 680-685.
- Landqvist, N. (1955). On the reaction between urea and formaldehyde in neutral and alkaline Solutions III experimental studies of the rates of hydrolysis of monomethylol urea. *Acta Chemica Scandinavica.* 9 (9): 1466-1470.
- Lobo, V., Patil, A., Phatak, A., Chandra, N. (2010). Free radicals, antioxidants and functional foods: Impact on human health. *Pharmacogn Rev.* 4 (8): 118-26.
- Lu, S.C. (2013). Glutathione synthesis. *Biochim Biophys Acta.* 1830 (5): 3143-53.
- Lu, S.C. (2009). Regulation of glutathione synthesis. *Mol Med.* 30 (1-2): 42-69.
- Luperchio, S., Tamir, S., Tannenbaum, S.R. (1996). NO-induced oxidative stress and glutathione metabolism in rodent and human cells. *Free Radic Biol Med.* 22 (4): 513-9.
- Mari, M., Morales, A., Colell, A., García-Ruiz, C., Fernández-Checa, J.C. (2009). Mitochondrial glutathione, a key survival antioxidant. *Antioxid Redox Signal.* 11(11): 2685-700.

Masella, R., Di Benedetto, R., Vari, R., Filesi, C., Giovannini, C. (2005). Novel mechanisms of natural antioxidant compounds in biological systems: involvement of glutathione and glutathione-related enzymes. *J Nutr Biochem.* 16 (10): 577-86.

Matthews, G.M., Butler, R.N. (2005). Cellular mucosal defense during *Helicobacter pylori* infection: a review of the role of glutathione and oxidative pentose pathway. *Helicobacter.* 10 (4): 298-306.

Mavis, R.D, Stellwagen, E. (1968). Purification and subunit structure of glutathione reductase from bakers' yeast. *J Biol Chem.* 243(4): 809-14.

Meyer, M., Schreck, R., Baeuerle, P. A. (1993). H₂O₂ and antioxidants have opposite effects on activation of NF-kappa B and AP-1 in intact cells: AP-1 as secondary antioxidant-responsive factor. *EMBO J.* 12 (5): 2005-15.

Morris, C.R., Suh, J.H., Hagar, W., Larkin, S., Bland, D.A., Steinberg, M.H., et al. (2008). Erythrocyte glutathione depletion, altered redox environment, and pulmonary hypertension in sickle cell disease. *Blood.* 111 (1): 402-10.

Morrison, J.L., Riggs, K.W., Rurak, D.W. (2005). Fluoxetine during pregnancy: impact on fetal development. *Reprod Fertil Dev.* 17 (6): 641-50.

Nojima, Y., Ito, K., Ono, H., Nakazato, T., Bono, H., Yokoyama, T. et al. (2015). Superoxide dismutase, SOD1 and SOD2, play a distinct role in the fat body during pupation in silkworm *Bombyx mori*. *PLoS One.* 10 (2): 1-20.

Nur, E., Biemond, B.J., Otten, H.M., Brandjes, D.P., Schnog, J.J. (2011). Oxidative stress in sickle cell disease; pathophysiology and potential implications for disease management. *Am J Hematol.* 86 (6): 484-9.

Ogüs, I.H., Ozer, N. (1998). Purification of NADPH-free glutathione disulfide reductase from human erythrocytes. *Protein Expr Purif.* 13 (1): 41-4.

Olschewski, A., Weir, E.K. (2015). Redox regulation of ion channels in the pulmonary circulation. *Antioxid Redox Signal.* 22 (6):465-85.

- Ortega, A.L., Mena, S., Estrela, J.M. (2011). Glutathione in cancer cell death. *Cancers (Basel)*. 3 (1): 1285-310.
- Outten, C.E., Culotta, V.C. (2004). Alternative start sites in *Saccharomyces cerevisiae* GLR1 gene are responsible for mitochondria and cytosolic isoforms of glutathione reductase. *J Biol Chem*. 279 (9): 7785-91.
- Pacher, P., Kecskemeti, V. (2004). Cardiovascular side effects of new antidepressants and antipsychotics: new drugs, old concerns? *Curr Pharm Des*. 10 (20): 2463-75.
- Pandey, K.B., Rizvi, S.I. (2010). Markers of oxidative stress in erythrocytes and plasma during aging in humans. *Oxid Med Cell Longev*. 3 (1): 2-12.
- Pannala, V.R., Bazil, J.N., Camara, A.K., Dash, R.K. (2013). A biophysically based mathematical model for the catalytic mechanism of glutathione reductase. *Free Radic Biol Med*. 65: 1385-97.
- Pannala, V.R., Bazil, J.N., Camara, A.K., Dash, R.K. (2014). A mechanistic mathematical model for the catalytic action of glutathione peroxidase. *Free Radic Res*. 48 (4): 487-502.
- Pham-Huy, L.A., He, H., Pham-Huy, C. (2008). Free radicals, antioxidants in disease and health. *Int J Biomed Sci*. 4 (2): 89-96.
- Pohland, R.C., Byrd, T.K., Hamilton, M., Koons, J.R. (1989). Placental transfer and fetal distribution of fluoxetine in rat. *Toxicol Appl Pharmacol*. 98 (2): 198-205.
- Queiroz, R.F., Lima, E.S. (2013). Oxidative stress in sickle cell disease. *Rev Bras Hematol Hemoter*. 35 (1): 16-7.
- Rahman, K., (2007). Studies on free radicals, antioxidants and co-factors. *Clin Interv Aging*. 2 (2): 219-36.
- Ray, A., Chatterjee, S., Mukherjee, S., Bhattacharya, S. (2014). Arsenic trioxide induced indirect and direct inhibition of glutathione reductase leads to apoptosis in rat hepatocytes. *Biometals*. 27 (3): 483-94.

Reuter, S., Gupta, S.C., Chaturvedi, M.M., Aggarwal, B.B. (2010). Oxidative stress, inflammation, and cancer: how are they linked? *Free Radic Biol Med.* 49 (11):1603-16.

Rietveld, P., Arscott, L.D., Berry, A., Scrutton, N.S., Deonarain, M.P., Perham, R.N. et al. (1994). Reductive and oxidative half-reactions of glutathione reductase from *Escherichia coli*. *Biochemistry.* 33 (46): 13888-95.

Ring, B.J., Eckstein, J.A., Gillespie, J.S., VandenBranden, M., Wrighton, S.A. (2001). Identification of the human cytochromes p450 responsible for in vitro formation of R- and S-norfluoxetine. *J Pharmacol Exp Ther.* 297 (3): 1044-50.

Rodríguez, V.M., Del.Razo, L.M., Limón-Pacheco, J.H., Giordano, M., Sánchez-peña, L.C., Uribe-Querol, E. et al. (2005). Glutathione reductase inhibition and methylated arsenic distribution in Cd1 mice brain and liver. *Toxicol Sci.* 84 (1): 157-66.

Rossi, A., Barraco, A., Donda, P. (2004). Fluoxetine: a review on evidence based medicine. *Ann Gen Hosp Psychiatry.*3(1): 2.

Salzman, C., Wolfson, A.N., Scatzberg, A., Looper, J., Henke, R., Albanese, M. et al. (1995). Effect of fluoxetine on anger in symptomatic volunteers with borderline personality disorder. *J Clin Psychopharmacol.* 15 (1): 23-9.

Sawyer, E.K., Howell, L.L. (2011). Pharmacokinetics of fluoxetine in rhesus macaques following multiple routes of administration. *Pharmacology.* 88 (1-2): 44-9.

Scordo, M.G., Spina, E., Dahl, M.L., Gatti, G., Perrucca, E. (2005). Influence of CYP2C9, 2C19 and 2D6 genetic polymorphisms on the steady-state plasma concentrations of the enantiomers of fluoxetine and norfluoxetine. *Basic Clin Pharmacol Toxicol.* 97 (5): 296-301.

Segel, I.R. (1975). *Enzyme Kinetics: Behaviour and Analysis of Rapid equilibrium and Steady-State Enzyme Systems.* New York: John Wiley and Sons Ins.

Sharma, R., Yang, Y., Sharma, A., Awasthi, S., Awasthi, Y.C. (2004). Antioxidant role of glutathione S- transferase: protein against oxidant toxicity and regulation of stress mediated apoptosis. *Antioxid Redox Signal.* 6 (2): 289-300.

Singh, A., Garg, V., Gupta, S., Kulkarni, S.K. (2002). Role of antioxidants in chronic fatigue syndrome in mice. *Indian J Exp Biol.* 40 (11): 1240-4.

Su, F., Hu, X., Jia, W., Gong, C., Song, E., Hamar, P. (2003). Glutathione-S-transferase pi indicates chemotherapy resistance in breast cancer. *J Surg Res.* 133 (1): 102-8.

Subramaniam, S.R., Chesselet, M.F. (2013). Mitochondrial dysfunction and oxidative stress in Parkinson's disease. *Prog Neurobiol.* 106-107: 17-32.

Tandogan, B., Güvenç, A., Caliş, İ., Ulusu, N.N. (2011). In vitro effects of compounds isolated from *Sideritis brevibracteata* on bovine kidney cortex glutathione reductase. *Acta Biochim Pol.* 58 (4): 471-5.

Tokarz, P., Kaarnivanta, K., Blasiak, J. (2013). Role of antioxidant enzymes and small molecular weight antioxidants in the pathogenesis of age related macular degeneration (AMD). *Biogerontology.* 14 (5): 461-82.

Toppo, S., Flohe, L., Vanin, S., Maiorino, M., (2009). Catalytic mechanisms and specificities of glutathione peroxidases: variations of a basic scheme. *Biochim Biophys Acta.* 1790 (11): 1486-500.

Townsend, D.M., Tew, K.D., Tapiero, H. (2003). The importance of glutathione in human disease. *Biomed Pharmacother.* 57 (3-4): 145-55.

Townsend, D.M., Tew, K.D. (2003). The role of glutathione-S-transferase in anti-cancer drug resistance. *Oncogene.* 22 (47): 7369-75.

Traverso, N., Ricciarelli, R., Nitti, M., Marengo, B., Furfaro, A. L., Pronzato, M. A et al., (2013). Role of glutathione in cancer progression and chemoresistance. *Oxid Med Cell Longev.* 2013: 972913.

Valko, M., Leibfritz, D., Moncol, J., Cronin, M.T., Mazur, M., Telser, J. (2007). Free radicals and antioxidants in normal physiological functions and human disease. *Int J Biochem Cell Biol.* 39 (1): 44-84.

Valko, M., Rhodes, C.J., Moncol, J., Izakovic, M., Mazur, M. (2006). Free radicals, metals and antioxidants in oxidative stress-induced cancer. *Chem Biol Interact.* 160 (1): 1-40.

Waggiallah, H., Alzohairy, M. (2011). The effect of oxidative stress on human red cells glutathione peroxidase, glutathione reductase level, and prevalence of anemia among diabetics. *N Am J Med Sci.* 3 (7): 344-7.

Wang, J., Zhang, Y., Xu, H., Zhu, S., Wang, H., HE, J. (2004). Fluoxetine improves behavioural performance by suppressing the production of soluble β -amyloid in APP/PS1 mice. *Curr Alzheimer Res.* 11 (7): 672-80.

Weydert, C.J., Cullen, J.J. (2010). Measurement of superoxide dismutase, catalase and glutathione peroxidase in cultured cells and tissue. *Nat Protoc.* 5 (1): 51-66.

Wilson, C.M. (1979). Studies and critique of Amido Black 10B, Coomassie Brilliant Blue R and fast Green FCF as stains for proteins after polyacrylamide gel electrophoresis. *Anal Biochem,* 96 (2): 263-273.

Wu, G., Fang, Y.Z., Yang, S., Lupton, J.R., Turner, N.D. (2004). Glutathione reductase metabolism and its implication for health. *J Nutr.* 134 (3): 489-92.

Xu, J.J., Chang, M.J., Yang, Y.C. (2011). Fluoxetine as treatment for post-traumatic stress disorder. *Neurosciences (Riyadh).* 16 (3): 257-62.

Yakes, F.M., Van Houten, B. (1997). Mitochondrial DNA damage is more extensive and persists longer than nuclear DNA damage in human cells following oxidative stress. *Proc Natl Acad Sci USA.* 94 (2): 514-9.

Zhao, Y., Seedfeldt, T., Chen, W., Carlson, L., Stoebner, A., Hanson, S., et al. (2009). Increase in thiol oxidative stress via glutathione reductase inhibition as a novel approach to enhance cancer sensitivity to X-ray irradiation. *Free Radic Biol Med.* 47(2): 176-183.